16 Specific Models

16.1 Preliminaries

There have been many studies of weak decays in concrete NP models. Here we want to describe in some detail only three classes of them:

- The so-called 331 models in which FCNC transitions are governed by a heavy Z' gauge boson with couplings that are more specific than in a general Z' scenario considered in Section 15.4.
- Models with vector-like quarks and leptons, that is new heavy fermions of which left-handed and right-handed components transform in the same manner under the SM gauge group. In simplest models the FCNC processes are dominated by tree-level Z exchanges and in certain models in addition by box diagrams with vector-like fermions and the Higgs boson. In more complicated models also other new heavy particles, in particular heavy gauge bosons and scalars can be present.
- Leptoquark models in which FCNC processes are dominated by the exchanges of heavy scalar or vector leptoquarks that directly couple quarks to leptons.

The reason for choosing these three classes of models is that they exhibit three different patterns of BSM flavor violation with different particles mediating FCNC processes. Moreover, they play some role in the explanation of the existing anomalies. But there are several other models that in principle deserve to be described here. Yet, in view of space limitations, we will only refer to three reviews [208, 870, 1000] in which I participated, and I will list the models and corresponding FCNC analyses of those that have been briefly described there. In particular in each case flavor properties of these models are listed, and in most cases Feynman rules (FR) for a given model are given. Also references to the relevant original papers can be found there. I would recommend to start with [208] and read the other two subsequently to appreciate that this field is very rich and changing with time. We have then:

- 2HDM$_{\overline{\text{MFV}}}$ model [896], which we briefly described in Section 15.2.
- Littlest Higgs Model with T-parity (LHT) [700] and without it (LH) [1001]. In both papers FR can be found.
- The SM with sequential fourth generation [1002].
- Supersymmetric flavor models that contain fewer parameters than the general MSSM [529].
- Supersymmetric SU(5) GUT model with right-handed neutrinos [1003].

Downloaded from https://www.cambridge.org/core. UNIVERSIDAD AUTONOMA METROPOLITANA, on 16 Nov 2026 at 12:03:57, subject to the Cambridge Core terms of use, available at https://www.cambridge.org/core/terms. https://doi.org/10.1017/9781139524100.022

- Supersymmetric SO(10) GUT model [1004].
- Flavor-blind MSSM [890].
- The minimal effective model with right-handed currents [610].
- Universal extra dimensions [1005, 1006], where FR are given.
- Randall–Sundrum model with custodial protection [920, 1007, 1008], where FR are given. See also [922, 1009–1011].
- Left-right symmetric models [772], where FR are given.
- Gauged flavor models [1012], where FR are given.
- Minimal theory of fermion masses with vector-like fermions [1013].
- Composite Higgs and partial compositeness. See [614, 1014–1017] and references to the original papers therein.
- Part III of the book [7] contains a lot of information on multi-Higgs doublet models, spontaneous CP violation, massive neutrinos and CPV in the leptonic sector, and strong CP problem, which we did not cover here. Also some additional information about vector-like quarks and some basics of left-right symmetric models can be found there.

16.2 331 Models

16.2.1 Introduction

Until now we have considered simplified models in which a single new heavy-gauge boson or a single scalar was added to the SM spectrum. In this section we will consider the so-called 331 models based on the gauge group $SU(3)_C \times SU(3)_L \times U(1)_X$ [1018, 1019], that is at first spontaneously broken to the SM group $SU(3)_C \times SU(2)_L \times U(1)_Y$ and then undergoes the spontaneous symmetry breaking to $SU(3)_C \times U(1)_Q$. The extension of the gauge group with respect to SM leads to a number of interesting consequences. The first one is that the requirement of anomaly cancellation together with that of asymptotic freedom of QCD implies that the number of generations must necessarily be equal to the number of colors, hence giving an explanation for the existence of three generations. But this is only possible if quark generations transform differently under the action of $SU(3)_L$. In particular, two quark generations should transform as triplets, one as an antitriplet. Choosing the latter to be the third generation, this different treatment could be at the origin of the large top quark mass. This choice imposes that the leptons should transform as antitriplets. However, one could choose a different scenario in which the role of triplets and antitriplets is exchanged, provided that the number of triplets equals that of antitriplets, to fulfill the anomaly cancellation requirement. Therefore, different versions of the model are obtained according to the way one fixes the fermion representations. Here we will consider two such representations called F_1 and F_2, which we will specify in the next subsection. This section is based on a series of papers [190, 613, 615, 852, 853] where more details can be found.

In these models a fundamental relation holds among the diagonal generators of the gauge group:

$$Q = T_3 + \beta T_8 + X, \tag{16.1}$$

Downloaded from https://www.cambridge.org/core. UNIVERSIDAD AUTONOMA METROPOLITANA, on 16 Nov 2026 at 12:03:57, subject to the Cambridge Core terms of use, available at https://www.cambridge.org/core/terms. https://doi.org/10.1017/9781139524100.022

where Q is the electric charge generator, T_3 and T_8 are two diagonal generators of the $SU(3)_L$, and X is the generator of $U(1)_X$. β is a key parameter that defines a specific variant of the model. The 331 models comprise several new particles, in particular a heavy Z' that is related to the generator of $U(1)_X$. There are moreover new heavy neutral and charged gauge bosons Y and V related to new generators present in $SU(3)_L$ beyond those of the SM $SU(2)_L$, a subgroup of $SU(3)_L$. Moreover, there are new heavy fermions, all with electric charges depending on β. Also the Higgs system is extended. But our discussion will concentrate dominantly on Z' as we would like to apply the technology developed in the previous chapter to a concrete model. Various properties of the remaining new particles are discussed in [613].

As described in detail in [1020], β could be in principle arbitrary. But as stressed in [613] only values

$$|\beta| \leq \sqrt{3} \tag{16.2}$$

are allowed. This follows from the fact that in 331 models

$$M_{Z'}^2 = \frac{g_2^2 u^2 c_W^2}{3[1-(1+\beta^2)s_W^2]}\,, \tag{16.3}$$

where u is the vacuum expectation value related to the first symmetry breaking and $s_W = \sin\vartheta_W$. It is then evident that only values of β satisfying

$$[1-(1+\beta^2)s_W^2] > 0 \tag{16.4}$$

are allowed. With the known value of s_W^2 this implies (16.2), and in fact the only explicit models analyzed in the literature are the ones with

$$\beta = \pm\frac{n}{\sqrt{3}}, \qquad n = 0, 1, 2, 3. \tag{16.5}$$

For $n = 1$ there are singly charged $Y^\pm$ bosons and neutral ones $V^0(\bar{V}^0)$, while for $n = 3$ one finds instead two new singly charged bosons $V^\pm$ and two doubly charged ones $Y^{\pm\pm}$. For $n = 2$ exotic charges $\pm 1/2$ and $\pm 3/2$ for gauge bosons are found. From table 1 in [613] we also find that while for $n = 1$ no exotic charges for heavy fermions are present, for $n = 2$ heavy quarks carry exotic electric charges $\pm 5/6$ and $\pm 7/6$, while heavy leptons $\pm 1/2$ and $\pm 3/2$. Discovering such fermions at the LHC would be a spectacular event. We refer to [613] for further details. In principle β could be a continuous variable satisfying (16.2), but in the present section we will only consider the cases $n = 1, 2$. The case $n = 3$ implies Landau singularities already at the LHC scales [190, 1021], while the model with $n = 0$, proposed in [1022], turns out to imply very small NP effects [853].

Most important for our discussion for all β, a new neutral gauge boson Z' is present, which as discussed in Section 15.4 and also in this section could help to explain various anomalies in several observables in $b \to s\mu^+\mu^-$ transitions. Compared with the general case of a Z' boson, the flavor-violating and flavor-conserving couplings are given in terms of fundamental parameters of a given 331 model, and consequently there is much less freedom in describing the data than in general Z' models. We will list these couplings in the next subsection.

Downloaded from https://www.cambridge.org/core. UNIVERSIDAD AUTONOMA METROPOLITANA, on 16 Nov 2026 at 12:03:57, subject to the Cambridge Core terms of use, available at https://www.cambridge.org/core/terms. https://doi.org/10.1017/9781139524100.022

Finally, a full description of flavor violation should take into account $Z - Z'$ mixing and implied flavor-violating contributions mediated by tree-level Z exchanges. We will describe these effects soon.

16.2.2 Parameters and Couplings

As in the SM, quark mass eigenstates are defined upon rotation of flavor eigenstates through two unitary matrices U_L (for up-type quarks) and V_L (for down-type quarks). The relation

$$V_{\rm CKM} = U_L^\dagger V_L \tag{16.6}$$

holds in analogy with the SM case. However, while in the SM $V_{\rm CKM}$ appears only in charged current interactions and the two rotation matrices never appear individually, this is not the case in this model, and both U_L and V_L can generate tree-level FCNCs mediated by Z' in the up-quark and down-quark sector, respectively. But these two matrices have to satisfy the relation (16.6). A useful parametrization for V_L proposed in [613] is

$$V_L = \begin{pmatrix} \tilde{c}_{12}\tilde{c}_{13} & \tilde{s}_{12}\tilde{c}_{23}e^{i\delta_3} - \tilde{c}_{12}\tilde{s}_{13}\tilde{s}_{23}e^{i(\delta_1-\delta_2)} & \tilde{c}_{12}\tilde{c}_{23}\tilde{s}_{13}e^{i\delta_1} + \tilde{s}_{12}\tilde{s}_{23}e^{i(\delta_2+\delta_3)} \\ -\tilde{c}_{13}\tilde{s}_{12}e^{-i\delta_3} & \tilde{c}_{12}\tilde{c}_{23} + \tilde{s}_{12}\tilde{s}_{13}\tilde{s}_{23}e^{i(\delta_1-\delta_2-\delta_3)} & -\tilde{s}_{12}\tilde{s}_{13}\tilde{c}_{23}e^{i(\delta_1-\delta_3)} - \tilde{c}_{12}\tilde{s}_{23}e^{i\delta_2} \\ -\tilde{s}_{13}e^{-i\delta_1} & -\tilde{c}_{13}\tilde{s}_{23}e^{-i\delta_2} & \tilde{c}_{13}\tilde{c}_{23} \end{pmatrix}. \tag{16.7}$$

This matrix implies through (16.6) new sources of flavor violation in the up-sector, but they will not be discussed here. However, when $U_L = \mathbb{1}$, as used in [1021], $V_L = V_{\rm CKM}$, and we deal with a particular simple CMFV model. In this book we would like to be more general, and V_L is given by (16.7).

With this parametrization, denoting the elements of the matrix V_L in (16.7) by v_{ij}, the Z' couplings to quarks, for the three meson systems, K, B_d, and B_s

$$\Delta_L^{sd}(Z'), \qquad \Delta_L^{bd}(Z'), \qquad \Delta_L^{bs}(Z'), \tag{16.8}$$

being proportional to $v_{32}^* v_{31}$, $v_{33}^* v_{31}$, and $v_{33}^* v_{32}$, respectively, depend only on four new parameters:

$$\boxed{\tilde{s}_{13}, \quad \tilde{s}_{23}, \quad \delta_1, \quad \delta_2.} \tag{16.9}$$

Here $\tilde{s}_{13}$ and $\tilde{s}_{23}$ are positive definite and δ_i in the range $[0, 2\pi]$. As $\tilde{s}_{13}$ and $\tilde{s}_{23}$ must be very small to satisfy flavor constraints, we have within an excellent approximation [613]

$$\boxed{v_{32}^* v_{31} = \tilde{s}_{13}\tilde{s}_{23}e^{i(\delta_2-\delta_1)}, \qquad v_{33}^* v_{31} = -\tilde{s}_{13}e^{-i\delta_1}, \qquad v_{33}^* v_{32} = -\tilde{s}_{23}e^{-i\delta_2}.} \tag{16.10}$$

Therefore, for fixed $M_{Z'}$ and β, the Z' contributions to all processes in the down-quark sector depend only on the four parameters in (16.9), implying very strong correlations between NP contributions to various observables. Indeed, as seen in (16.10), the B_d system involves only the parameters $\tilde{s}_{13}$ and δ_1 while the B_s system depends on $\tilde{s}_{23}$ and δ_2. Moreover, stringent correlations between observables in $B_{d,s}$ sectors and in the kaon sector

Downloaded from https://www.cambridge.org/core. UNIVERSIDAD AUTONOMA METROPOLITANA, on 16 Nov 2026 at 12:03:57, subject to the Cambridge Core terms of use, available at https://www.cambridge.org/core/terms. https://doi.org/10.1017/9781139524100.022

are found because kaon physics depends on $\tilde{s}_{13}$, $\tilde{s}_{23}$, and $\delta_2 - \delta_1$. A very constraining feature of this model is that the diagonal couplings of Z' to quarks and leptons are fixed for a given β, except for a weak dependence on $M_{Z'}$ due to running of $\sin^2\vartheta_W$ provided β differs significantly from $\pm\sqrt{3}$, which is satisfied for $n = 1, 2$ in (16.5).

It follows that $\tilde{s}_{13}$ and δ_1 can be determined from ΔM_d and CP-asymmetry $S_{\psi K_S}$ while $\tilde{s}_{23}$ and δ_2 from ΔM_s and CP-asymmetry $S_{\psi\phi}$. Then the parameters in the K system are fixed.

We will now recall Z' couplings to SM fermions for arbitrary β concentrating on those that are relevant for this book. The expressions for other couplings and masses of new gauge bosons and fermions as well as expressions for their electric charges that depend on β can be found in [613].

The fundamental quantity that enters all couplings is the function

$$f(\beta) = \frac{1}{1 - (1+\beta^2)s_W^2} > 0, \tag{16.11}$$

where the positivity of this function results from the reality of $M_{Z'}$ as stressed earlier.

The following properties should be noted:

- For $\beta \approx \sqrt{3}$ there is a Landau singularity for $s_W^2 = 0.25$. As at M_W one has $s_W^2 \approx 0.23$ (with exact number depending on its definition considered) and renormalization group evolution of weak couplings increases s_W^2 with increasing scale, $s_W^2(M_{Z'})$ reaches 0.25, and the singularity in question for $M_{Z'} \approx 4\,\text{TeV}$.
- For $|\beta| \leq \sqrt{3} - 0.20$ this problem does not arise even up to the GUT scales.

While we will specifically consider only the cases $\beta = \pm n/\sqrt{3}$ with $n = 1, 2$, we list here the formulas for the relevant couplings for arbitrary real $\beta \neq \sqrt{3}$ satisfying (16.2). The case $\beta = \sqrt{3}$ is considered in an appendix in [190].

We stress that the couplings of Z' to quarks and leptons have to be evaluated at the scale μ at which Z' is integrated out, that is at $\mu = O(M_{Z'})$ and not at M_W. For $n = 1$ this difference is irrelevant. For $n = 2$ it plays a role if acceptable precision is required, and it is crucial for $n = 3$. The numerical values of couplings listed following are collected in an appendix in [190].

The relevant Z' couplings to quarks are then given as follows:

$$\Delta_L^{ij}(Z') = \frac{g}{\sqrt{3}} c_W \sqrt{f(\beta)} v_{3i}^* v_{3j}, \tag{16.12a}$$

$$\Delta_L^{ji}(Z') = \left[\Delta_L^{ij}(Z')\right]^*, \qquad \Delta_L^{u\bar{u}}(Z') = \Delta_L^{d\bar{d}}(Z'), \tag{16.12b}$$

$$\Delta_L^{d\bar{d}}(Z') = \frac{g}{2\sqrt{3}c_W}\sqrt{f(\beta)}\left[-1 + \left(1 + \frac{\beta}{\sqrt{3}}\right)s_W^2\right], \tag{16.12c}$$

$$\Delta_R^{u\bar{u}}(Z') = \frac{g}{2\sqrt{3}c_W}\sqrt{f(\beta)}\frac{4}{\sqrt{3}}\beta s_W^2 = -2\Delta_R^{d\bar{d}}(Z'), \tag{16.12d}$$

$$\Delta_V^{d\bar{d}}(Z') = \frac{g}{2\sqrt{3}c_W}\sqrt{f(\beta)}\left[-1 + \left(1 - \frac{\beta}{\sqrt{3}}\right)s_W^2\right], \tag{16.12e}$$

Downloaded from https://www.cambridge.org/core. UNIVERSIDAD AUTONOMA METROPOLITANA, on 16 Nov 2026 at 12:03:57, subject to the Cambridge Core terms of use, available at https://www.cambridge.org/core/terms. https://doi.org/10.1017/9781139524100.022

$$\Delta_A^{d\bar{d}}(Z') = \frac{g}{2\sqrt{3}c_W}\sqrt{f(\beta)}\left[1-\left(1+\sqrt{3}\beta\right)s_W^2\right], \tag{16.12f}$$

$$\Delta_V^{u\bar{u}}(Z') = \frac{g}{2\sqrt{3}c_W}\sqrt{f(\beta)}\left[-1+\left(1+\frac{5}{\sqrt{3}}\beta\right)s_W^2\right], \tag{16.12g}$$

$$\Delta_A^{u\bar{u}}(Z') = \frac{g}{2\sqrt{3}c_W}\sqrt{f(\beta)}\left[1-\left(1-\sqrt{3}\beta\right)s_W^2\right], \tag{16.12h}$$

where v_{ij} are the elements of the matrix V_L in (16.7). The diagonal couplings are valid for the first two generations of quarks neglecting the very small nondiagonal contributions in the matrices V_L and U_L. For the third generation there is an additional term that can be found in [613].

For leptons we have

$$\Delta_L^{\nu\bar{\nu}}(Z') = \frac{g}{2\sqrt{3}c_W}\sqrt{f(\beta)}\left[1-\left(1+\sqrt{3}\beta\right)s_W^2\right], \tag{16.13a}$$

$$\Delta_L^{\mu\bar{\mu}}(Z') = \Delta_L^{\nu\bar{\nu}}(Z'), \tag{16.13b}$$

$$\Delta_R^{\mu\bar{\mu}}(Z') = \frac{-g\,\beta\,s_W^2}{c_W}\sqrt{f(\beta)}, \tag{16.13c}$$

$$\Delta_V^{\mu\bar{\mu}}(Z') = \frac{g}{2\sqrt{3}c_W}\sqrt{f(\beta)}\left[1-\left(1+3\sqrt{3}\beta\right)s_W^2\right], \tag{16.13d}$$

$$\Delta_A^{\mu\bar{\mu}}(Z') = \frac{g}{2\sqrt{3}c_W}\sqrt{f(\beta)}\left[-1+\left(1-\sqrt{3}\beta\right)s_W^2\right]. \tag{16.13e}$$

Until now we discussed only flavor-violating couplings of Z', but in the process of electroweak symmetry breaking $Z-Z'$ mixing takes place implying that there is a small mixing between Z and Z' so that the heavy mass eigenstates are really

$$Z_\mu^1 = \cos\xi\, Z_\mu + \sin\xi\, Z'_\mu, \qquad Z_\mu^2 = -\sin\xi\, Z_\mu + \cos\xi\, Z'_\mu. \tag{16.14}$$

Here Z_μ is the mass eigenstate in the SM, and Z' is the gauge boson corresponding to the generator of $\mathrm{U}(1)_X$. For $\sin\xi = 0$ the two mass eigenstates are simply $Z_\mu^1 = Z_\mu$ and $Z_\mu^2 = Z'_\mu$. Consequently only Z'_μ has flavor-violating couplings in the mass eigenstate basis for quarks as a result of different transformation properties of the third generation under the extended gauge group.

When the small but nonvanishing mixing represented by $\sin\xi$ is taken into account, not only the flavor-violating couplings of the mass eigenstate Z_μ^1 to quarks are generated but also its flavor-diagonal couplings to SM fermions differ from the ones of the SM Z boson. Explicitly we have for $i \neq j$

$$\Delta_L^{ij}(Z^1) = \sin\xi\,\Delta_L^{ij}(Z') \equiv \Delta_L^{ij}(Z), \qquad \Delta_L^{ij}(Z^2) = \cos\xi\,\Delta_L^{ij}(Z') \approx \Delta_L^{ij}(Z'), \tag{16.15}$$

where in order not to modify the notation in flavor-violating observables relative to the previous chapter, we will still use Z for Z^1 and Z' for Z^2 with masses M_Z and $M_{Z'}$, respectively. The small shifts in the masses of these gauge bosons relative to the case $\sin\xi = 0$ are irrelevant in flavor-violating processes.

Downloaded from https://www.cambridge.org/core. UNIVERSIDAD AUTONOMA METROPOLITANA, on 16 Nov 2026 at 12:03:57, subject to the Cambridge Core terms of use, available at https://www.cambridge.org/core/terms. https://doi.org/10.1017/9781139524100.022

For flavor-diagonal couplings to fermions (generically denoted with f), we have with $k = L, R, A, V$

$$\Delta_k^{ff}(Z^1) = \cos\xi\, \Delta_k^{ff}(Z) + \sin\xi\, \Delta_k^{ff}(Z'), \tag{16.16}$$

$$\Delta_k^{ff}(Z^2) = \cos\xi\, \Delta_k^{ff}(Z') - \sin\xi\, \Delta_k^{ff}(Z). \tag{16.17}$$

In the calculations of flavor-violating effects we can neglect the mixing effects in these couplings so that we can simply set

$$\Delta_k^{ff}(Z^1) = \Delta_k^{ff}(Z), \qquad \Delta_k^{ff}(Z^2) = \Delta_k^{ff}(Z'), \tag{16.18}$$

but in the analysis of electroweak precision tests, performed in [615], one has to keep mixing effects in (16.16).

As the mass M_Z and flavor-diagonal Z-couplings to all SM fermions are known, the model is also predictive after the inclusion of $Z - Z'$ mixing, although one additional parameter, $\tan\bar{\beta}$, enters the game. This mixing has been calculated correctly first in [615] with the result

$$\boxed{\sin\xi = \frac{c_W^2}{3}\sqrt{f(\beta)}\left(3\beta\frac{s_W^2}{c_W^2} + \sqrt{3}a\right)\left[\frac{M_Z^2}{M_{Z'}^2}\right]}, \tag{16.19}$$

where $f(\beta)$ is given in (16.11) and

$$-1 < a = \frac{v_-^2}{v_+^2} < 1, \tag{16.20}$$

with $v_\pm^2$ given in terms of the vacuum expectation values of two Higgs triplets ρ and η present in these models as follows

$$v_+^2 = v_\eta^2 + v_\rho^2, \qquad v_-^2 = v_\eta^2 - v_\rho^2. \tag{16.21}$$

As the Higgs system responsible for the breakdown of the SM group has the structure of a two Higgs doublet model and the triplets ρ and η are responsible for the masses of up-quarks and down-quarks, respectively, one can, express the parameter a in terms of the usual $\tan\bar{\beta}$ where we introduced a *bar* to distinguish the usual angle β from the parameter β in 331 models. We have then

$$a = \frac{1 - \tan^2\bar{\beta}}{1 + \tan^2\bar{\beta}}, \qquad \tan\bar{\beta} = \frac{v_\rho}{v_\eta}. \tag{16.22}$$

Thus for $\tan\bar{\beta} = 1$ the parameter $a = 0$, which simplifies the formula for $\sin\xi$ relating uniquely its sign to the sign of β. On the other hand, in the large $\tan\bar{\beta}$ limit we find $a = -1$ and in the low $\tan\bar{\beta}$ limit one has $a = 1$.

The expression in (16.19) tells us definitely that $\sin\xi$ is very small but one should remember that the propagator suppression of FCNC transitions in the case of Z' is by a factor of $M_{Z'}^2/M_Z^2$ stronger than in the case of Z at the amplitude level. Therefore a more detailed numerical analysis of the values of $\sin\xi$ and Z' couplings to leptons as functions of β and $\tan\bar{\beta}$ and the comparison with the known Z couplings to fermions is required to

Downloaded from https://www.cambridge.org/core. UNIVERSIDAD AUTONOMA METROPOLITANA, on 16 Nov 2026 at 12:03:57, subject to the Cambridge Core terms of use, available at https://www.cambridge.org/core/terms. https://doi.org/10.1017/9781139524100.022

decide whether Z boson contributions to FCNC processes can be neglected or not. Such an analysis has been performed in [615], and we will report on its outcome later. However, first we have to elaborate on the choice of fermion representations.

16.2.3 Choice of Fermion Representations

It has been emphasized in [1020, 1023] that the choice of β does not uniquely specify the phenomenology of the 331 model considered, which further depends on the choice of fermion representations under $SU(3)_L$. Here we will discuss two choices for which a detailed analysis has been presented in [615].

In the first choice, to be denoted by F_1, and used exclusively in [190, 613], the first two generations of quarks are put into triplets (3), while the third one into the antitriplet (3^*):

$$\begin{pmatrix} u \\ d \\ D \end{pmatrix}_L, \qquad \begin{pmatrix} c \\ s \\ S \end{pmatrix}_L, \qquad \begin{pmatrix} b \\ -t \\ T \end{pmatrix}_L. \tag{16.23}$$

The corresponding right-handed quarks are singlets. The anomaly cancellation then requires that leptons are put into antitriplets:

$$\begin{pmatrix} e \\ -\nu_e \\ E_e \end{pmatrix}_L, \qquad \begin{pmatrix} \mu \\ -\nu_\mu \\ E_\mu \end{pmatrix}_L, \qquad \begin{pmatrix} \tau \\ -\nu_\tau \\ E_\tau \end{pmatrix}_L. \tag{16.24}$$

On the other hand, as done in [1020, 1023], the triplets and antitriplets are interchanged relative to F_1. That is, the first two quark generations are in antitriplets while the third one in a triplet. Therefore leptons are also in triplets. We will call this fermion assignment F_2. In [1020, 1023] still two other quark assignments are discussed in which the first or the second quark generation transforms differently under $SU(3)_L$ than the remaining two. But we find the ones just listed more natural due to large top-quark mass, and we do not discuss these two additional possibilities.

The important two features are the following ones. For a given β:

- The expression for $\sin\xi$ in (16.19) is independent of whether F_1 or F_2 is used.
- On the other hand the signs in front of β in Z' couplings to quarks and leptons are changed when going from F_1 to F_2. This property can be derived from the action of the relevant operator $\hat{Q}_W$ on triplet and antitriplet. See formulas in section 2 of [613]. This can also be seen by comparing Z' couplings to fermions, given for F_1, with table 4 of [1023], where the couplings are given for F_2.

As pointed out in [615] these properties have the following important phenomenological implications listed here first without FCNC mediated by the Z boson:

- In F_1 scenario the models with $\beta = -2/\sqrt{3}$ and $\beta = -1/\sqrt{3}$ are useful for the explanation of the anomalies in $B_d \to K^*\mu^+\mu^-$ because with F_1 representations the coupling $\Delta_V^{\mu\tilde{\mu}}(Z')$ is large. On the other hand, the models with $\beta = 2/\sqrt{3}$ and $\beta = 1/\sqrt{3}$ having significant $\Delta_A^{\mu\tilde{\mu}}(Z')$ coupling provide interesting NP effects in $B_{s,d} \to \mu^+\mu^-$.

Downloaded from https://www.cambridge.org/core. UNIVERSIDAD AUTONOMA METROPOLITANA, on 16 Nov 2026 at 12:03:57, subject to the Cambridge Core terms of use, available at https://www.cambridge.org/core/terms. https://doi.org/10.1017/9781139524100.022

- In F_2 scenario the situation is reversed. The models with $\beta = 2/\sqrt{3}$ and $\beta = 1/\sqrt{3}$ are useful for the explanation of the anomalies in $B_d \to K^*\mu^+\mu^-$, while the ones with $\beta = -2/\sqrt{3}$ and $\beta = -1/\sqrt{3}$ for $B_{s,d} \to \mu^+\mu^-$.
- While these two scenarios cannot be distinguished by flavor observables when only Z' contributions are considered, they can be distinguished when Z boson contributions are taken into account. This originates in the fact that the $\sin\xi$ entering the $\Delta_L^{ij}(Z)$ couplings in (16.15) *does depend* on the sign of β but *does not depend* on whether F_1 scenario or F_2 scenario is considered. In other words, the invariance in flavor observables under the transformations

$$\beta \to -\beta, \qquad F_1 \to F_2 \tag{16.25}$$

  present in the absence of $Z - Z'$ mixing is broken by this mixing. We will see this explicitly in our following discussion.
- As a particular sign of β could be favored by flavor-conserving observables, in particular electroweak precision tests, this feature allows in principle to determine whether the representation F_1 or F_2 is favored by nature. We will see this explicitly in the next subsection.

16.2.4 Distinguishing 331 Models through Electroweak Precision Tests

A detailed analysis of 24 models in question corresponding to different values of β and $\tan\bar{\beta}$ for the representations F_1 and F_2 has been presented in [615]. They are collected in Table 16.1. In particular a detailed analysis of electroweak precision tests in these models has been performed there. Interested readers are asked to look at section 5 of that paper. Here we just summarize the main outcome of that study.

Requiring that the 24 models in question perform at least as well as the SM in these tests, only seven models passed this test and have been selected for a more detailed study of FCNC processes. These are

$$\text{M9}, \quad \text{M8}, \quad \text{M6}, \quad \text{M11}, \quad \text{M3}, \quad \text{M16}, \quad \text{M14}, \quad \text{(favored)}, \tag{16.26}$$

Table 16.1 Definition of the various 331 models.

MI	scen.	β	$\tan\bar{\beta}$	MI	scen.	β	$\tan\bar{\beta}$	MI	scen.	β	$\tan\bar{\beta}$
M1	F_1	$-2/\sqrt{3}$	1	M9	F_2	$-2/\sqrt{3}$	1	M17	F_1	$-2/\sqrt{3}$	0.2
M2	F_1	$-2/\sqrt{3}$	5	M10	F_2	$-2/\sqrt{3}$	5	M18	F_2	$-2/\sqrt{3}$	0.2
M3	F_1	$-1/\sqrt{3}$	1	M11	F_2	$-1/\sqrt{3}$	1	M19	F_1	$-1/\sqrt{3}$	0.2
M4	F_1	$-1/\sqrt{3}$	5	M12	F_2	$-1/\sqrt{3}$	5	M20	F_2	$-1/\sqrt{3}$	0.2
M5	F_1	$1/\sqrt{3}$	1	M13	F_2	$1/\sqrt{3}$	1	M21	F_1	$1/\sqrt{3}$	0.2
M6	F_1	$1/\sqrt{3}$	5	M14	F_2	$1/\sqrt{3}$	5	M22	F_2	$1/\sqrt{3}$	0.2
M7	F_1	$2/\sqrt{3}$	1	M15	F_2	$2/\sqrt{3}$	1	M23	F_1	$2/\sqrt{3}$	0.2
M8	F_1	$2/\sqrt{3}$	5	M16	F_2	$2/\sqrt{3}$	5	M24	F_2	$2/\sqrt{3}$	0.2

Downloaded from https://www.cambridge.org/core. UNIVERSIDAD AUTONOMA METROPOLITANA, on 16 Nov 2026 at 12:03:57, subject to the Cambridge Core terms of use, available at https://www.cambridge.org/core/terms. https://doi.org/10.1017/9781139524100.022

with the first five performing better than the SM, while the last two basically as the SM. The models with *odd* index I correspond to $\tan\bar{\beta} = 1.0$ and the ones with *even* one to $\tan\bar{\beta} = 5.0$. The models with $\tan\bar{\beta} = 0.2$ did not pass these tests, which is unfortunate, as only these models among all models considered could give significant contributions to rare decays $K^+ \to \pi^+\nu\bar{\nu}$ and $K_L \to \pi^0\nu\bar{\nu}$.

16.2.5 Summary of FCNC Results

Extensive flavor analyses in 331 models can be found in [190, 613, 615, 852, 853]. References to earlier analysis of flavor physics in 331 models can be found there and in [1020, 1023].

The most recent updated analyses in [852, 853] concentrated on the ratio ε'/ε and its correlation with ε_K and B-physics observables like $\Delta M_{s,d}$, $B_s \to \mu^+\mu^-$, and the Wilson coefficient C_9. They were motivated by the anomalies in ε'/ε [244, 275, 276, 296], tension between ε_K and $\Delta M_{s,d}$ within the SM [388] implied by the lattice data in [873], and in the case of C_9 by the LHCb anomalies in the angular observables in $B \to K^*(K)\mu^+\mu^-$ mentioned in Section 12.2.

We briefly summarize the main results of [852, 853]. These analyses show that the requirement of an enhancement of ε'/ε has a significant impact on other flavor observables. Moreover, in [853] it has also been shown that the results are rather sensitive to the value of $|V_{cb}|$, as has been illustrated there by choosing two values: $|V_{cb}| = 0.040$ and $|V_{cb}| = 0.042$. The main lessons extracted from [852, 853] for $M_{Z'} = 3$ TeV are as follows:

Lesson 1: Among the seven 331 models in (16.26), selected on the basis of the electroweak precision study, only three (M8, M9, M16) can provide for both choices of $|V_{cb}|$, significant shift of ε'/ε, even though not larger than 8×10^{-4}.

Lesson 2: The tensions between $\Delta M_{s,d}$ and ε_K pointed out in [388], see Section 15.1, can be removed in these models (M8, M9, M16) for both values of $|V_{cb}|$.

Lesson 3: In agreement with our previous expectations, two of them (M8 and M9) can simultaneously with the enhancement of ε'/ε suppress $B_s \to \mu^+\mu^-$ by at most 10% and 20% for $|V_{cb}| = 0.042$ and $|V_{cb}| = 0.040$, respectively. This is presently sufficient for bringing the theory close to the central experimental value. On the other hand, the maximal deviations from SM in the Wilson coefficient C_9 are $C_9^{\rm NP} = -0.1$ and $C_9^{\rm NP} = -0.2$ for these two $|V_{cb}|$ values, respectively. Due to this moderate shift, these models do not really help in the case of $B_d \to K^*\mu^+\mu^-$ anomalies that require deviations as high as $C_9^{\rm NP} = -1.0$.

Lesson 4: In M16 the situation is reversed. It is possible to reduce the rate for $B_s \to \mu^+\mu^-$ for $M_{Z'} = 3$ TeV for the two $|V_{cb}|$ values by at most 3% and 10%, respectively. With the corresponding values $C_9^{\rm NP} = -0.3$ and -0.5, the anomaly in $B_d \to K^*\mu^+\mu^-$ can be significantly reduced.

Lesson 5: The maximal shifts in ε'/ε decrease fast with increasing $M_{Z'}$ in the case of $|V_{cb}| = 0.042$ but are practically unchanged for $M_{Z'} = 10$ TeV when $|V_{cb}| = 0.040$ is used.

Lesson 6: On the other hand, for larger values of $M_{Z'}$ the effects in $B_s \to \mu^+\mu^-$ and $B_d \to K^*\mu^+\mu^-$ are much smaller. NP effects in rare K decays and $B \to K(K^*)\nu\bar{\nu}$ remain small in all 331 models even for $M_{Z'}$ of few TeV. This could be challenged by NA62, KOTO, and Belle II experiments in this decade.

Downloaded from https://www.cambridge.org/core. UNIVERSIDAD AUTONOMA METROPOLITANA, on 16 Nov 2026 at 12:03:57, subject to the Cambridge Core terms of use, available at https://www.cambridge.org/core/terms. https://doi.org/10.1017/9781139524100.022

All these results are illustrated in numerous plots in [852, 853].

Finally, we return to the outcome of general analyses of B-physics anomalies from which, as we saw in Section 12.2, the most favorite relations between NP contributions to C_9 and C_{10} were before Moriond 2019

$$C_9^{\rm NP} = -C_{10}^{\rm NP} = -0.62 \pm 0.12 \quad \text{or} \quad C_9^{\rm NP} = -1.0 \pm 0.2, \;\; C_{10}^{\rm NP} = 0. \tag{16.27}$$

These relations should be contrasted with models M8 and M9 for which one finds [852]

$$C_9^{\rm NP} = 0.49\, C_{10}^{\rm NP} \quad \text{(M8)}, \qquad C_9^{\rm NP} = 0.42\, C_{10}^{\rm NP} \quad \text{(M9)}. \tag{16.28}$$

Thus as already seen earlier, models M8 and M9 have significant problems with the observed pattern of these anomalies. On the other hand,

$$C_9^{\rm NP} = -4.59\, C_{10}^{\rm NP} \quad \text{(M16)} \tag{16.29}$$

is close to the second relation in (16.27) where NP resides dominantly in the coefficient C_9. Thus already on the basis of B physics observables, we should be able to distinguish between the three favorite 331 models M8, M9, and M16.

The messages from Moriond 2019 did not change this pattern, and presently M16 appears to be in the best shape, but we have to wait for improved data to have a clear-cut conclusion. In particular as the RH FCNC are absent in 331 models; this could be another problem for these models if the presence of RH currents, proposed by several authors as a solution to the anomalies in question, will be established.

Thus the main message from [852, 853] is that NP contributions in 331 models can simultaneously solve $\Delta F = 2$ tensions, enhance ε'/ε, and suppress either the rate for $B_s \to \mu^+\mu$ or C_9 Wilson coefficient without any significant effect on $K^+ \to \pi^+\nu\bar{\nu}$ and $K_{\rm L} \to \pi^0\nu\bar{\nu}$ and $b \to s\nu\bar{\nu}$ transitions. While sizable NP effects in $\Delta F = 2$ observables and ε'/ε can persist for $M_{Z'}$ outside the reach of the LHC, such effects in $B_s \to \mu^+\mu^-$ will only be detectable provided Z' will be discovered soon. The future of 331 models will also depend on the fate of the violation of flavor lepton universality hinted at by the data as these models cannot explain it, although they can provide modifications in C_9 and C_{10} as just discussed.

We did not review lepton physics in 331 models. We refer to [1024], where a good collection of relevant references and phenomenology of lepton decays in a specific 331 model can be found.

16.3 Vector-Like Quarks and Leptons

16.3.1 Introduction

Presently we know that three generations of quarks and leptons exist. Their left-handed and right-handed components transform differently under the electroweak part of the SM gauge group, and only after this symmetry group is spontaneously broken can their masses be generated through their Yukawa couplings to the SM Higgs. We also know that the fourth

Downloaded from https://www.cambridge.org/core. UNIVERSIDAD AUTONOMA METROPOLITANA, on 16 Nov 2026 at 12:03:57, subject to the Cambridge Core terms of use, available at https://www.cambridge.org/core/terms. https://doi.org/10.1017/9781139524100.022

generation of quarks and leptons does not exist because otherwise LHC would have already discovered them, and also the required large Yukawa coupling to Higgs would imply much larger Higgs width than measured. But heavy fermions with left-handed and right-handed components transforming identically under the SM gauge group can exist because the generation of their masses does not require spontaneous breakdown of electroweak symmetry (SSB). They can even be so heavy that the LHC cannot discover them directly in collisions. Yet, we should still hope that the LHC will see them in the coming years.

The masses of these vector-like fermions can be generated by some mechanism at very short-distance scales that we do not have to specify at the time being. We can just add the corresponding mass term to the SM Lagrangian by hand and specify how these new heavy fermions interact with SM particles. Such fermions will be termed vector-like fermions (VLFs), vector-like quarks (VLQs), and vector-like leptons (VLLs). This section deals with flavor physics of these new heavy particles, which this time carry spin-1/2 as opposed to the spin-1 gauge boson Z' and heavy scalars with spin-0.

In fact, among the simplest renormalizable extensions of the SM that do not introduce any additional fine-tunings of parameters are models in which the only new particles are VLFs. As already stated such fermions can be much heavier than the SM fermions as they can acquire masses in the absence of electroweak SSB. But if in the process of this breaking they can mix with ordinary fermions, the most natural implication is the generation of FCNC processes mediated by the SM Z boson. We will first discuss this simplest situation concentrating on VLQs, postponing the extension of the SM group by a U(1) factor to the second part of this section. With a new heavy gauge boson Z' and new heavy scalars necessary to provide Z' mass and to break the extended gauge symmetry group down to the SM gauge group, the models with VLFs are more involved but are also interesting.

There is a rich literature on FCNC implied by the presence of VLQs. See in particular [783, 792, 925, 967, 1025–1032]. Here we will be guided by the analysis in [666], which analyzed the patterns of flavor violation in a number of VLQ models classified in [783, 784, 967]. The latter authors identified all renormalizable models with additional fermions residing in a single vector-like complex representation of the SM gauge group with a mass M. It turns out that there are 11 models where new fermions have proper quantum numbers so that they can couple in a renormalizable manner to the SM Higgs and SM fermions, thereby implying new sources of flavor violation.

In this section our discussion will be confined to FCNC in K, B_d, and B_s systems, and only five of these models will be relevant for us. They will be specified in Section 16.3.2. We will see that in these models Yukawa interactions of the SM scalar doublet H involving ordinary quarks and VLQs imply flavor-violating Z couplings to ordinary quarks. In this manner VLQ models are explicit realizations of Z models discussed in Section 15.5 with various flavor-violating couplings of Z given in terms of Yukawa couplings and VLQ masses.

NP contributions to $\Delta F = 1$ FCNC transitions are then dominated by tree-level Z exchanges. The pattern of NP contributions to $\Delta F = 2$ processes is more involved. Indeed, as pointed out in [967], for the masses of VLQs $M \geq 5\,\text{TeV}$ NP contributions to $\Delta F = 2$ transitions from box diagrams with VLQs and Higgs become very important. This property will modify the correlation between $\Delta F = 1$ and $\Delta F = 2$ processes encountered in

Downloaded from https://www.cambridge.org/core. UNIVERSIDAD AUTONOMA METROPOLITANA, on 16 Nov 2026 at 12:03:57, subject to the Cambridge Core terms of use, available at https://www.cambridge.org/core/terms. https://doi.org/10.1017/9781139524100.022

Z-models discussed in Section 15.5. But in [967] the contributions from Yukawa RG effects discussed in Section 15.5 have not been taken into account. As we have seen, there these effects depend on whether RH or LH flavor-violating quark couplings to the Z are present. If they are RH, the effects of RG evolution from M (the common VLQ mass) down to the electroweak scale, $\mu_{\rm ew}$, generate left-right operators [766] via top-Yukawa induced mixing. These operators are strongly enhanced through QCD RG effects below the electroweak scale and in the case of the K system through chirally enhanced hadronic matrix elements. They dominate then NP contributions to ε_K, but in the $B_{s,d}$ meson systems for VLQ-masses above 5 TeV they have to compete with contributions from box diagrams with VLQs mentioned earlier. If they are LH the Yukawa enhancement is less important because left-right operators are not present, and box diagrams play an important role both in the $B_{s,d}$ and K systems.

Now NP contributions to flavor observables in K, B_d, and B_s systems depend in each model, respectively, on the products of complex Yukawa couplings $\lambda_s^*\lambda_d$, $\lambda_b^*\lambda_d$, and $\lambda_b^*\lambda_s$ and the common VLQ mass M. This structure allows to set one of the phases to zero so that each model depends on five Yukawa parameters and M, implying a number of correlations between flavor observables not only within a given meson system but also between those in different meson systems. This goes beyond the Z scenario of Section 15.5, where there was no relation between different meson systems.

The outline of this section is as follows. In the next subsection we will summarize the particle content of the five VLQ models considered by us together with gauge interactions and Yukawa interactions. Subsequently we will discuss the decoupling of VLQs both at tree-level and one-loop level. Next phenomenology of these models will be presented. We will close this section by describing briefly what happens in VLQ models in which the gauge group is extended by a U(1) factor, a heavy gauge boson Z' is present, and the scalar sector contains new heavy scalars beyond the SM Higgs. This section is dominantly based on [666], where further details and references to rich literature can be found.

16.3.2 The VLQ Models

VLQ Representations

We will focus on models with VLQs residing in complex representations of the SM gauge group. We adapt the usual SM fermion content of the three generations ($i = 1,2,3$) of quarks ($q_L^i = (u_L^i, d_L^i)^T, u_R^i, d_R^i$) and leptons ($L_L^i = (\nu_i, \ell_L^i)^T, \ell_R^i$), which acquire masses via spontaneous symmetry breaking from the standard scalar $\mathrm{SU(2)_L}$ doublet H.

As we are mainly interested in the phenomenlogy of down-quark physics, we will restrict our analysis to $\mathrm{SU(3)}_C$ triplets and consider the following five models with $\mathrm{SU(2)_L}$ singlets, doublets, and triplets

$$\begin{aligned}
&\text{Singlets}: && D(1,-1/3), && && \text{(V)} && \text{(LH)} \\
&\text{Doublets}: && Q_V(2,+1/6), && Q_d(2,-5/6), && \text{(IX, XI)} && \text{(RH)} \\
&\text{Triplets}: && T_d(3,-1/3), && T_u(3,+2/3), && \text{(VII, VIII)} && \text{(LH)},
\end{aligned} \tag{16.30}$$

Downloaded from https://www.cambridge.org/core. UNIVERSIDAD AUTONOMA METROPOLITANA, on 16 Nov 2026 at 12:03:57, subject to the Cambridge Core terms of use, available at https://www.cambridge.org/core/terms. https://doi.org/10.1017/9781139524100.022

where the transformation properties are indicated as $(\mathrm{SU}(2)_\mathrm{L}, \mathrm{U}(1)_\mathrm{Y})$. The representations D, Q_V, Q_d, T_d, and T_u correspond to the models V, IX, XI, VII, and VIII introduced in [967]. Already at this stage we indicated which models bring in new LH currents and which RH currents. We will be more explicit about it later. The kinetic and gauge interactions of the new VLQs are given by

$$\mathcal{L}_\mathrm{kin} = \overline{D}(i\not{\mathcal{D}} - M_D)D + \sum_{a=V,d} \overline{Q}_a(i\not{\mathcal{D}} - M_{Q_a})\,Q_a + \sum_{a=d,u} \mathrm{Tr}\left[\overline{T}_a(i\not{\mathcal{D}} - M_{T_a})\,T_a\right], \quad (16.31)$$

with appropriate covariant derivatives $\mathcal{D}_\mu$, and we follow [967] for the triplet representations as given in (2.13) and (2.14) of that paper. The masses M of the VLQs introduce a new scale, which we will assume throughout to be significantly larger than the electroweak scale. Typical at least $O(1\ \mathrm{TeV})$ as required by the LHC bounds. The covariant derivative is, omitting the $\mathrm{SU}(3)_C$ part,

$$\mathcal{D}_\mu = \partial_\mu - ig_2\frac{\sigma^a}{2}W^a_\mu - ig_1 Y B_\mu, \quad (16.32)$$

with the SM gauge couplings $g_{1,2}$ and σ^a being Pauli matrices.

Yukawa Interactions of VLQs

The scalar sector contains only the standard doublet $H(2,+1/2)$, with its usual scalar potential. It provides masses to gauge bosons and standard fermions in the course of electroweak SSB via the VEV $v \simeq 246$ GeV, where

$$\langle H\rangle = (0, v/\sqrt{2})^T. \quad (16.33)$$

The VLQs interact with SM quarks (q_L, u_R, d_R) via Yukawa interactions

$$\begin{aligned} -\mathcal{L}_\mathrm{Yuk}(H) = &\left(\lambda^D_i\, H^\dagger \overline{D}_R + \lambda^{T_d}_i\, H^\dagger \overline{T}_{dR} + \lambda^{T_u}_i\, \widetilde{H}^\dagger \overline{T}_{uR}\right) q^i_L \\ &+ \lambda^{V_u}_i\, \bar{u}^i_R \widetilde{H}^\dagger Q_{VL} + \bar{d}^i_R \left(\lambda^{V_d}_i\, H^\dagger Q_{VL} + \lambda^{Q_d}_i\, \widetilde{H}^\dagger Q_{dL}\right) + \mathrm{h.c.}, \end{aligned} \quad (16.34)$$

where $\widetilde{H} \equiv i\sigma_2 H^*$. The complex-valued Yukawa couplings λ^VLQ_i with $i = 1,2,3$ or equivalently in the models considered $i = d, s, b$ give rise to mixing with the SM quarks and flavor-changing Z-couplings, which have been worked out in detail [967] and confirmed up to one sign in T_u model in [666]. We will be more explicit in Section 16.3.3.

16.3.3 Decoupling of VLQs

Preliminaries

The VLQ models are characterized by the masses M of the VLQs and the various Yukawa couplings λ^VLQ_i $(i = 1,2,3)$ listed earlier. The present lower bound on M from the LHC is in the ballpark of 1 TeV.

Downloaded from https://www.cambridge.org/core. UNIVERSIDAD AUTONOMA METROPOLITANA, on 16 Nov 2026 at 12:03:57, subject to the Cambridge Core terms of use, available at https://www.cambridge.org/core/terms. https://doi.org/10.1017/9781139524100.022

We have thus the hierarchy

$$m_b \ll v \ll M. \tag{16.35}$$

It is then natural to decouple first VLQs and to consider an effective theory valid between scales $\mu_M \sim M$ and $\mu_{\rm EW} \sim v$ and subsequently match it to the effective $\mathrm{SU}(3)_C \otimes \mathrm{U}(1)_{em}$ theory valid between $\mu_{\rm EW}$ and $\mu_b \sim m_b$. Here m_b denotes the mass of the bottom quark, which is the heaviest of the light standard particles. This will indicate which operators are most important. The evolution to lower scales relevant for K meson physics is done as in previous chapters.

In this subsection we present the results from the decoupling of the VLQs that are important for phenomenological applications within the framework of the LEFT relevant for weak decays of mesons. The decoupling proceeds either by explicit matching calculations starting at tree-level and including subsequently higher orders or by integrating VLQs out in the path integral method [783]. The tree-level decoupling is known for a long time [783]. The one-loop decoupling has been presented in [967] and confirmed up to small differences in [666].

The VLQs have a very limited set of couplings to light fields, which are either via gauge interactions (16.31) to the gauge bosons or via Yukawa interactions (16.34) to light – w.r.t. to VLQ mass M – SM quarks. At tree-level, this particular structure of interactions can give rise only to flavor-changing (FC) Z couplings, whereas all other decoupling effects are loop-suppressed.

The decoupling of the VLQs proceeds in the unbroken phase of $\mathrm{SU}(2)_L \otimes \mathrm{U}(1)_Y$, hence quark fields are flavor-eigenstates, and neutral components of SM Higgs doublet are without VEV at this stage. After the RG-evolution from μ_M to $\mu_{\rm EW}$, SSB will take place, and the transformation from flavor- to mass-eigenstates for fermions and gauge bosons can be performed.

A detailed discussion of this decoupling has been presented in [666, 783, 967], but we will only present the results following the presentation in [666].

Tree-Level Decoupling and Z Interactions

As discussed in detail in [666] the relation of quark masses to Yukawa interactions includes now also $1/M^2$ contributions, and their diagonalization proceeds as usual for the quark fields with the help of 3×3 unitary rotations

$$\psi_L \to V_L^{\psi} \psi_L, \qquad \psi_R \to V_R^{\psi} \psi_R \tag{16.36}$$

in flavor space, implying

$$V_L^{\psi\dagger} m_\psi V_R^{\psi} = m_\psi^{\rm diag}, \qquad V = (V_L^u)^\dagger V_L^d \tag{16.37}$$

that is diagonal up- and down-quark masses $m_\psi^{\rm diag}$ and the quark-mixing matrix V (CKM matrix). Throughout our discussion we will assume that down quarks are already mass eigenstates, which fixes also the basis for the VLQ Yukawa couplings $\lambda_i^{\rm VLQ}$ and implies $q_L = (V^\dagger u_L, d_L)^T$.

Downloaded from https://www.cambridge.org/core. UNIVERSIDAD AUTONOMA METROPOLITANA, on 16 Nov 2026 at 12:03:57, subject to the Cambridge Core terms of use, available at https://www.cambridge.org/core/terms. https://doi.org/10.1017/9781139524100.022

Table 16.2 $\Delta^{ij}_{L,R}(Z)$ for $i,j = d,s,b$ in VLQ models.

Coupling	D	Q_V	Q_d	T_d	T_u
$\Delta^{ij}_L(Z)$	Δ^{ij}	0	0	$\Delta^{ij}/2$	$-\Delta^{ij}$
$\Delta^{ij}_R(Z)$	0	$-(\Delta^{ij})^*$	$(\Delta^{ij})^*$	0	0

After SSB flavor-changing Z interactions for fermions ($f = \ell, d, u$) are generated. We parametrize them as in Section 15.5 through

$$\mathcal{L}^{(Z)}_{\rm VLQ} = \bar{f}^i \left[\Delta^{ij}_L(Z)\,\gamma^\mu P_L + \Delta^{ij}_R(Z)\,\gamma^\mu P_R\right] f^j Z_\mu. \tag{16.38}$$

The flavor-diagonal couplings of Z to quarks and leptons will be set to the ones of the SM as corrections from NP to them are fully negligible. Thus flavor-diagonal Z couplings to fermions are universal for all models considered. On the other hand, flavor-violating couplings are model dependent.

The decoupling of VLQs, presented in details in [666], gives the results for $\Delta_{L,R}(Z)$ couplings collected for down-quarks in Table 16.2, where

$$\Delta^{ij} \equiv \frac{\lambda_i^*\lambda_j}{g_Z}\frac{M_Z^2}{M^2}, \qquad\qquad g_Z \equiv \sqrt{g_1^2+g_2^2}. \tag{16.39}$$

Except for the sign in the case of T_u, the results of [666] agree with those in [967]. Further, also nonzero couplings to up-type quarks arise [967], but they will not be investigated in this book.

Decoupling at One-Loop Level

All other decoupling processes proceed via loops. They turn out to be relevant only for $\Delta F = 2$ processes. VLQs contribute then to the Wilson coefficients of the by-now-familiar $|\Delta F| = 2$ operators O_a^{ij} for $a = {\rm VLL}, {\rm VRR}, {\rm LR1}$ via box diagrams that contain two heavy VLQ propagators with representations F_m and F_n and massless components of the standard doublet $H = (H^+, H^0)^T$. The resulting Wilson coefficients have the following general structure

$$C_a^{ij} = \frac{\eta_{mn}}{(4\pi)^2}\frac{\Lambda^m_{ij}\Lambda^n_{ij}}{\mathcal{N}_{ij}} f_1(M_m, M_n), \qquad \mathcal{N}_{ij} = \frac{G_F^2}{4\pi^2} M_W^2 (\lambda_t^{ji})^2 \tag{16.40}$$

at the scale μ_M. Here the prefactor $\mathcal{N}_{ij}$ corresponds to the SM normalization of the $|\Delta F| = 2$ Hamiltonian. The function

$$f_1(M_m, M_n) = \frac{\ln(M_m^2/M_n^2)}{M_m^2 - M_n^2} \qquad \text{with} \qquad f_1(M_m, M_m) = \frac{1}{M_m^2}, \tag{16.41}$$

Downloaded from https://www.cambridge.org/core. UNIVERSIDAD AUTONOMA METROPOLITANA, on 16 Nov 2026 at 12:03:57, subject to the Cambridge Core terms of use, available at https://www.cambridge.org/core/terms. https://doi.org/10.1017/9781139524100.022

Table 16.3 The index a = VLL, VRR, LR1 appearing in (16.40) for representations (F_m, F_n), followed by corresponding η_{mn}.

(F_m, F_n)	D	Q_d	Q_V	T_d	T_u
D	VLL, +1/8	LR1, +1/4	LR1, −1/4	VLL, +1/16	VLL, −1/8
Q_d		VRR, +1/4	VRR, −1/4	LR1, +3/8	LR1, −3/8
Q_V			VRR, +1/4	LR1, −3/8	LR1, +3/8
T_d				VLL, +5/32	VLL, −1/8
T_u					VLL, +5/32

depends on the VLQ masses of representations $F_{m,n}$. The couplings Λ_{ij}^m are

$$\Lambda_{ij}^m = (\lambda_i^m)^* \lambda_j^m \qquad \text{for} \qquad F_m = D, T_d, T_u, \tag{16.42}$$

$$\Lambda_{ij}^m = \lambda_i^m (\lambda_j^m)^* \qquad \text{for} \qquad F_m = Q_d, Q_V. \tag{16.43}$$

The index a of the operator and the numerical factors η_{mn} are collected in Table 16.3. Note that a = VLL for $F_{m,n} = D, T_d, T_u$, and a = VRR for $F_{m,n} = Q_d, Q_V$, whereas a = LR1 for $F_m = D, T_d, T_u$ and $F_n = Q_d, Q_V$. The factors η_{mn} are positive except for interference of $F_m = D, Q_d, T_d$ with $F_n = Q_V, T_u$, because in this case the scalar propagators are crossed, which gives rise to an additional sign w.r.t. the diagram with noncrossed scalar propagators. For $F_m = F_n$, these results agree with [967] for D, T_u, T_d, but for Q_d (model XI), we find an additional factor of 2. Concerning Q_V (model IX), we find a contribution to $\sim O_{\text{VRR}}$ instead of $\sim O_{\text{VLL}}$ and also opposite sign. For completeness we provide also the results for $F_m \neq F_n$.

Before discussing the Yukawa RG effects, let us compare the relative size of box-to-Z exchange contribution to the box function S that we encountered in previous chapters. With the information collected so far and the formulas for tree-level Z contributions of Section 15.5, we readily find

$$\frac{(\Delta S)_{\text{Box}}}{(\Delta S)_Z} = a\, \eta_{LL} \frac{g_Z^2}{8\pi^2} \left[\frac{\tilde{r}_{\text{Box}}}{\tilde{r}_Z}\right] \frac{M^2}{M_Z^2} \tag{16.44}$$

with $a = 4$ for T_d and unity otherwise. $r_{\text{Box}} \approx \tilde{r}_Z \approx 1$. Moreover, as seen in Table 16.3 $\eta_{LL} = (1/8, 1/4, 5/32)$ for D, (Q_d, Q_V) and (T_d, T_u), respectively. While the Z contribution is comparable to the box contribution for $M \approx 1 - 2$ TeV, it amounts only to a few percent for $M = 10$ TeV. This is not surprising. While to box contributions are dimension-6 contributions to the effective Hamiltonian, the tree-level Z contributions correspond to dimension-8 operators.

The presence of box diagrams modifies the correlation between $|\Delta F| = 2$ and $|\Delta F| = 1$ observables relative to Section 15.5. But to complete the analysis, we have to discuss the RG effects. The ones from QCD alone have been already included in the estimates earlier but we will recall them next. The ones related to Yukawa couplings are more involved, and we will discuss them in more detail.

Downloaded from https://www.cambridge.org/core. UNIVERSIDAD AUTONOMA METROPOLITANA, on 16 Nov 2026 at 12:03:57, subject to the Cambridge Core terms of use, available at https://www.cambridge.org/core/terms. https://doi.org/10.1017/9781139524100.022

QCD Renormalization Group Evolution

For $|\Delta F| = 2$ the QCD evolution from μ_M to $\mu_{\rm EW}$ involves only $N_f = 6$ and is given at LO as follows [744]

$$\begin{aligned} C_{\rm VLL,VRR}(\mu_{\rm EW}) &= \eta_6^{2/7} C_{\rm VLL,VRR}(\mu_M), \\ C_{\rm LR,1}(\mu_{\rm EW}) &= \eta_6^{1/7} C_{\rm LR,1}(\mu_M), \\ C_{\rm LR,2}(\mu_{\rm EW}) &= \frac{2}{3}\left(\eta_6^{1/7} - \eta_6^{-8/7}\right) C_{\rm LR,1}(\mu_M) + \eta_6^{-8/7} C_{\rm LR,2}(\mu_M), \end{aligned} \tag{16.45}$$

with $\eta_6 = \alpha_s^{(6)}(\mu_M)/\alpha_s^{(6)}(\mu_{\rm EW})$. Initial conditions of $C_a^{ij}(\mu_M)$ resulting from box diagrams are collected in (16.40). Note that $C_{\rm LR,1}(\mu_M) \neq 0$ only in the presence of several VLQ representations, but always $C_{\rm LR,2}(\mu_M) = 0$. Renormalization group evolution for tree-level Z contributions starts at $\mu_{\rm EW}$.

Yukawa Renormalization Group Effects

These effects have been already formulated in the framework of SMEFT in Section 14.4. To use these results we have to calculate the coefficients of dimension-6 operators in VLQ models in question at the scale μ_M of order of the VLQ masses. Such a calculation has been done in [783] and confirmed in [666]. We have then

$$\begin{aligned} D: &\quad [C_{Hq}^{(1)}]_{ij} = [C_{Hq}^{(3)}]_{ij} = -\frac{1}{4}\frac{\lambda_i^*\lambda_j}{M^2}, \\ T_d: &\quad [C_{Hq}^{(1)}]_{ij} = -3\,[C_{Hq}^{(3)}]_{ij} = -\frac{3}{8}\frac{\lambda_i^*\lambda_j}{M^2}, \\ T_u: &\quad [C_{Hq}^{(1)}]_{ij} = 3\,[C_{Hq}^{(3)}]_{ij} = \frac{3}{8}\frac{\lambda_i^*\lambda_j}{M^2}, \\ Q_d: &\quad [C_{Hd}]_{ij} = -\frac{1}{2}\frac{\lambda_i\lambda_j^*}{M^2}, \\ Q_V: &\quad [C_{Hd}]_{ij} = \frac{1}{2}\frac{\lambda_i^{V_d}\lambda_j^{V_d*}}{M^2}, \quad [C_{Hu}]_{ij} = -\frac{1}{2}\frac{\lambda_i^{V_u}\lambda_j^{V_u*}}{M^2}, \quad [C_{Hud}]_{ij} = \frac{\lambda_i^{V_u}\lambda_j^{V_d*}}{M^2}. \end{aligned} \tag{16.46}$$

Using these results and the technology of Section 14.4, we find the contributions to the Wilson coefficients of $\Delta F = 2$ operators from the Yukawa RG effects

$$C_a^{ij}(\mu_{\rm ew}) = \frac{\kappa_m}{(4\pi)^2}\frac{\Lambda_{ij}^m \lambda_{ij}^{(t)}}{\mathcal{N}_{ij}}\frac{1}{M^2}\frac{2m_t^2}{v^2}\ln\frac{\mu_M}{\mu_{\rm ew}}, \tag{16.47}$$

Downloaded from https://www.cambridge.org/core. UNIVERSIDAD AUTONOMA METROPOLITANA, on 16 Nov 2026 at 12:03:57, subject to the Cambridge Core terms of use, available at https://www.cambridge.org/core/terms. https://doi.org/10.1017/9781139524100.022

with Λ_{ij}^m in (16.42) and (16.43), the chirality of the $|\Delta F| = 2$ operator

$$\begin{aligned} a &= \text{VLL} \qquad \text{for} \qquad F_m = D, T_d, T_u, \\ a &= \text{LR}, 1 \qquad \text{for} \qquad F_m = Q_d, Q_V, \end{aligned} \tag{16.48}$$

and the VLQ-model-dependent factor

$$\kappa_m = \left(0,\ -\frac{1}{2},\ +\frac{1}{2},\ -\frac{1}{2},\ +\frac{1}{4}\right) \qquad \text{for} \qquad F_m = (D,\ Q_d,\ Q_V,\ T_d,\ T_u). \tag{16.49}$$

We note the relations

$$\kappa_m \frac{\Lambda_{ij}^m}{M^2} = [C_{Hq}^{(1)} - C_{Hq}^{(3)}]_{ij}, \qquad (F_m = D,\ T_d,\ T_u), \tag{16.50}$$

and

$$\kappa_m \frac{\Lambda_{ij}^m}{M^2} = [C_{Hd}]_{ij}, \qquad (F_m = Q_d,\ Q_V). \tag{16.51}$$

We point out the different flavor structure of the 1stLLA contribution (16.47) compared to the one of the direct box contribution (16.40) discussed previously:

$$C_a^{ij}|_{\text{1stLLA}} \ \sim\ \Lambda_{ij} \times \lambda_{ij}^{(t)}, \qquad\qquad C_b^{ij}|_{\text{Box}} \ \sim\ (\Lambda_{ij})^2, \tag{16.52}$$

showing linear versus quadratic dependence on the product of VLQ Yukawa couplings Λ_{ij}.

Yukawa RG Effects versus Box Contributions

With only the box and tree-level Z contributions taken into account the $|\Delta F| = 2$ observables are not sensitive to the chirality of the VLQ interactions as long as only one VLQ representation is present. However, the inclusion of RG Yukawa effects just presented and NLO contributions discussed in [766] changes this picture drastically in the case of VLQ models with flavor-changing RH currents (Q_d, Q_V) and has also significant impact in the remaining three models with LH currents.

In the case of D, T_d, and T_u models, we find

$$\left[\frac{(\Delta S)_{\text{RG}}}{(\Delta S)_{\text{Box}}}\right]^{ij} = \frac{\kappa_m}{\eta_{mm}} \frac{\lambda_{ij}^t}{\Lambda_{ij}^m} \frac{2m_t^2}{v^2 \eta_6^{2/7}} \left[\ln \frac{\mu_M}{\mu_{\text{EW}}} + \frac{F_{\text{NLO}}(x_t, \mu_{\text{EW}})}{\kappa_m \Lambda_{ij}^m}\right], \tag{16.53}$$

with κ_m given in (16.49) and η_{mm} in Table 16.3. The NLO correction

$$\begin{aligned} F_{\text{NLO}}(x_t, \mu_{\text{EW}}) = {} & [C_{Hq}^{(1)}]_{ij} H_1(x_t, \mu_{\text{ew}}) - [C_{Hq}^{(3)}]_{ij} H_2(x_t, \mu_{\text{ew}}) \\ & + \frac{2S_0(x_t)}{x_t} \sum_m \left(\lambda_t^{im} [C_{Hq}^{(3)}]_{mj} + [C_{Hq}^{(3)}]_{im} \lambda_t^{mj}\right) \end{aligned} \tag{16.54}$$

has been calculated in [766], where also the x_t-dependent functions $H_{1,2}$ can be found.

In the case of Q_d and Q_V models, the box and RG contributions yield coefficients to different operators, hence a meaningful comparison of their impact on observables has to

Downloaded from https://www.cambridge.org/core. UNIVERSIDAD AUTONOMA METROPOLITANA, on 16 Nov 2026 at 12:03:57, subject to the Cambridge Core terms of use, available at https://www.cambridge.org/core/terms. https://doi.org/10.1017/9781139524100.022

include their QCD running between $\mu_{\rm ew}$ and the light flavor scales (we choose 3 GeV for Kaons and M_B for $B_{d,s}$), as well as the corresponding matrix elements. We find

$$\left[\frac{(M_{12}^*)_{\rm RG}}{(M_{12}^*)_{\rm Box}}\right]^{ij} = \left[\frac{(M_{12}^*)_{\rm LR}}{(M_{12}^*)_{\rm VRR}^{\rm box}}\right]^{ij} = \frac{\kappa_m}{\eta_{mm}}\frac{\lambda_{ij}^t}{\Lambda_{ij}^m}\frac{2m_t^2}{v^2\eta_6^{2/7}}\left[\ln\frac{\mu_M}{\mu_{\rm EW}} + H_1(x_t,\mu_{\rm EW})\right] R^{ij}, \quad (16.55)$$

with R^{ij} including RG factors and the ratio of the hadronic matrix elements. From Eqs. (60) and (61) in [766], we obtain

$$R^{sd} \approx -80 \qquad \text{and} \qquad R^{b(d,s)} \approx -3. \quad (16.56)$$

This large chiral enhancement in the Kaon system renders the RG contribution dominant, while in the $B_{d,s}$ systems the contribution remains comparable with the box contribution.

16.3.4 Structure of the Phenomenology

The free parameters relevant for the study of K, B_s, and B_d meson systems in a given VLQ model are the complex Yukawa couplings:

$$\lambda_d, \quad \lambda_s, \quad (K), \quad (16.57)$$
$$\lambda_b, \quad \lambda_s, \quad (B_s), \quad (16.58)$$
$$\lambda_b, \quad \lambda_d, \quad (B_d) \quad (16.59)$$

and the mass M of the VLQs, which we assume to be common for all members of the VLQ multiplet.

Thus every model contains three complex Yukawa couplings:

$$\boxed{\lambda_d = |\lambda_d|e^{i\phi_d}, \qquad \lambda_s = |\lambda_s|e^{i\phi_s}, \qquad \lambda_b = |\lambda_b|e^{i\phi_b},} \quad (16.60)$$

which enter flavor observables in K, B_d, and B_s systems in the case of models with LH currents through three products

$$\Lambda_{sd} = \lambda_s^*\lambda_d = A_{sd}e^{-i\phi_{sd}}, \ \Lambda_{bd} = \lambda_b^*\lambda_d = A_{bd}e^{-i\phi_{bd}}, \ \Lambda_{bs} = \lambda_b^*\lambda_s = A_{bs}e^{-i\phi_{bs}}, \quad (16.61)$$

respectively. Here

$$\boxed{\phi_{ij} = \phi_i - \phi_j \quad \Rightarrow \quad \phi_{bs} = \phi_{bd} - \phi_{sd}.} \quad (16.62)$$

For models with RH currents just complex conjugation in the definition of Λ_{ij} has to be made. See (16.42) and (16.43).

The A_{ij} are positive definite real parameters, and the phases ϕ_{ij} can vary in the full range $[0, 2\pi]$. The latter fact implies discrete phase ambiguities when these phases are determined from experiment as explicitly seen in the plots in [611, 666]. As only the differences of phases are involved, without lost of generality, we can set one of them to zero. Setting then $\phi_d = 0$ we find

$$|\lambda_d| = \sqrt{\frac{A_{bd}A_{sd}}{A_{bs}}}, \qquad |\lambda_s| = \sqrt{\frac{A_{bs}A_{sd}}{A_{bd}}}, \qquad |\lambda_b| = \sqrt{\frac{A_{bs}A_{bd}}{A_{sd}}} \quad (16.63)$$

Downloaded from https://www.cambridge.org/core. UNIVERSIDAD AUTONOMA METROPOLITANA, on 16 Nov 2026 at 12:03:57, subject to the Cambridge Core terms of use, available at https://www.cambridge.org/core/terms. https://doi.org/10.1017/9781139524100.022

and

$$\phi_d = 0, \qquad \phi_s = \phi_{sd}, \qquad \phi_b = \phi_{bd}. \tag{16.64}$$

These couplings enter $|\Delta F| = 2$ observables, and one might expect strongest constraints on A_{sd} because of the strong suppression of the SM contribution by $V_{td}V_{ts}^*$, whereas λ_b in turn is constrained by $|\Delta B| = 2$ measurements.

In a sense the flavor structure of VLQ models has some parallels to the one in 331 models discussed in the previous section. However, in 331 models the NP contributions are dominated by Z' tree-level exchanges, and once the constraints from $B_{s,d}$ observables are taken into account, NP effects in the K system are found to be small, with the exception of ε'/ε. In VLQ models important Z boson contributions are present, and this allows for more interesting NP effects than in 331 models in $K^+ \to \pi^+\nu\bar{\nu}$ and $K_{\rm L} \to \pi^0\nu\bar{\nu}$, as we will see soon. Furthermore, the presence of important box diagram contributions to $|\Delta F| = 2$ processes and of Yukawa RG effects in VLQ models discussed earlier increases the impact of $|\Delta F| = 2$ constraints on $|\Delta F| = 1$ processes relative to the ones found in 331 models.

16.3.5 Patterns of NP in VLQ Models

We will now summarize various lessons gained from the extensive analysis of VLQ models in [666]. The interested readers will find numerous plots in this paper that show visually the patterns listed next. The patterns are similar to the ones encountered in Z scenarios of Section 15.5, but the models here are more concrete and allow some correlations between different meson systems.

Lesson 1: The VLQ models allow to enhance ε'/ε significantly, thereby addressing the apparent gap between the SM prediction and data, at the expense of suppressing $\mathcal{B}(K_{\rm L} \to \pi^0\nu\bar{\nu})$. This suppression is significantly weaker for Q_V and Q_d models (RH currents) than for D, T_d, and T_u (LH currents), in accordance with the general study in [851]. Simultaneous agreement with the data for ε_K and ε'/ε can be obtained without fine-tuning of parameters.

Lesson 2: While the impact of ε'/ε on $K_{\rm L} \to \pi^0\nu\bar{\nu}$ is large as just stated, $K^+ \to \pi^+\nu\bar{\nu}$ and ε'/ε are only weakly correlated. However, in RH models ϵ_K prevents large enhancements of $\mathcal{B}(K^+ \to \pi^+\nu\bar{\nu})$, the maximal enhancement is about 50% of its SM value. In models with LH currents, a strong suppression is possible, and the SM value corresponds to an upper bound in this case when a stricter bound from $K_L \to \mu\bar{\mu}$ is used. This implies that a measurement of a significantly enhanced $\mathcal{B}(K^+ \to \pi^+\nu\bar{\nu})$, as presently still allowed by data, could exclude all VLQ models with a single VLQ representation, although in models with LH currents a more conservative bound from $K_L \to \mu\bar{\mu}$ would presently still allow the enhancement of $\mathcal{B}(K^+ \to \pi^+\nu\bar{\nu})$ up to a factor of two. In this context it should be again emphasized that the modes $K^+ \to \pi^+\nu\bar{\nu}$ and $K_L \to \mu\bar{\mu}$ are strongly correlated in VLQ models, however, again differently so for LH and RH currents. While for RH currents one can easily infer the allowed range in one mode from a determination of the other, within the limited range allowed by ε'/ε and ϵ_K, LH-current models are more strongly constrained from $K_L \to \mu\bar{\mu}$. But there is basically no correlation

Downloaded from https://www.cambridge.org/core. UNIVERSIDAD AUTONOMA METROPOLITANA, on 16 Nov 2026 at 12:03:57, subject to the Cambridge Core terms of use, available at https://www.cambridge.org/core/terms. https://doi.org/10.1017/9781139524100.022

between ε'/ε and $K_L \to \mu\bar{\mu}$, as they are governed by imaginary and real parts of the corresponding couplings, respectively.

Lesson 3: The VLQ mass does not have a large impact on all these correlations, as can be seen in the plots in [666].

Moving then to $b \to s$ processes one finds.

Lesson 4: Because NP effects in all three quark transitions are governed by different parameters, the slight tensions in $|\Delta F| = 2$ observables hinted at by lattice data [873] can easily be removed in VLQ models. This is in contrast to constrained-MFV models, where ε_K prohibits large effects in $\Delta M_{d,s}$ [388].

Lesson 5: $\mathcal{B}(B_s \to \mu\bar{\mu})$ can be strongly suppressed below its SM value, as slightly favored by experiment, while still allowing for sizable NP effects in $\sin(2\beta_s)$, in particular in the case of models with LH currents. For $M_{\rm VLQ} = 1$ TeV $|\Delta F| = 1$ observables constrain the NP effects in ϕ_s to be smaller than for larger VLQ masses.

Lesson 6: Sizable deviations from the SM prediction are still possible for the mass-eigenstate rate asymmetry $A_{\Delta\Gamma}(B_s \to \mu\bar{\mu})$ and the mixing-induced CP-asymmetry $S^s_{\mu\mu}$. Indeed, both can essentially vary in the full range $[-1, 1]$ for LH models for $M_{\rm VLQ} = 1$ TeV. For RH models, $A_{\Delta\Gamma}(B_s \to \mu\bar{\mu}) \geq 50\%$ for $M_{\rm VLQ} = 1$ TeV, but still $|S^s_{\mu\mu}|$ can reach up to 80%. For $M_{\rm VLQ} = 10$ TeV, the former is restricted to positive values in both LH and RH models, the latter slightly stronger constrained in RH models, but not in LH ones.

Lesson 7: CP-violating quantities are almost 100% correlated in $b \to s$ transitions as long as only one representation is considered. The reason is that the SM predictions are tiny, and all NP contributions therefore directly proportional to the imaginary part of Λ_{bs}, which hence cancels in the ratio of two CP-violating quantities. For small NP contributions, the asymmetries are simply proportional to each other, for larger effects the relation depends on the normalization of the asymmetry. These statements hold not only in VLQ models, but in all models that provide only a single new phase in $b \to s$ transitions, only the proportionality constant changes in other models.

Lesson 8: Interesting CP-violating effects in various asymmetries due to imaginary parts of $b \to s\mu\bar{\mu}$ Wilson coefficients $C_{9,9',10,10'}$ have been identified. The correlations between these asymmetries provide transparent distinction between LH and RH currents.

Lesson 9: NP effects in $B \to K^{(*)}\nu\bar{\nu}$ turn out to be small in RH scenario. In LH scenario basically only suppression of branching ratios is possible.

Lesson 10: Similar to the case of Z models the anomalies in $b \to \ell^+\ell^-$ and $b \to c\tau\bar{\nu}_\tau$ cannot be explained in these models.

Having the latter anomalies in mind the paper [666] considered also VLQ models with an additional Z' related to $\mathrm{U}(1)_{L_\mu - L_\tau}$. Here the results depend on the Higgs system necessary to generate the mass of Z'. The main lessons are as follows.

Lesson 11: In a model with an additional singlet, as considered in [925], $b \to s\mu^+\mu^-$ anomalies can be partly explained by providing sufficient suppression of the coefficient C_9, but NP effects in $B_{s,d} \to \mu\bar{\mu}$ and $K_L \to \mu\bar{\mu}$ are absent, those in $b \to s\nu\bar{\nu}$ transitions small and the ones in $K^+ \to \pi^+\nu\bar{\nu}$ and $K_{\rm L} \to \pi^0\nu\bar{\nu}$ much smaller than in the VLQ models discussed earlier. Most important these models fail badly in explaining the ε'/ε anomaly. This pattern is related to the absence of FCNC processes mediated by Z and to pure vector coupling of Z' to charged leptons.

Downloaded from https://www.cambridge.org/core. UNIVERSIDAD AUTONOMA METROPOLITANA, on 16 Nov 2026 at 12:03:57, subject to the Cambridge Core terms of use, available at https://www.cambridge.org/core/terms. https://doi.org/10.1017/9781139524100.022

However, adding an additional scalar doublet Φ FCNC processes mediated by Z can be generated [666], and the patterns of NP are modified as we describe now.

Lesson 12: While the explanation of $b \to s\mu^+\mu^-$ anomalies is more difficult than in models just discussed, due to the presence of Z contributions interesting effects in other observables can be found. In particular, NP effects in ε'/ε *and* $K^+ \to \pi^+\nu\bar{\nu}$ can be large, in contrast to VLQ models based on the SM gauge group.

Lesson 13: NP effects in ΔM_K can be larger and correlated with $K^+ \to \pi^+\nu\bar{\nu}$. In particular if in the future the ΔM_K constraint will be improved, large enhancements of $\mathcal{B}(K^+ \to \pi^+\nu\bar{\nu})$ are likely to be excluded. On the other hand, NP effects in $K_{\rm L} \to \pi^0\nu\bar{\nu}$, $K_L \to \mu\bar{\mu}$, $B \to K(K^*)\nu\bar{\nu}$, and $B_{d,s} \to \mu\bar{\mu}$ are very small and beyond the reach of even presently planned future facilities.

Thus if NP will be found in $B_{s,d} \to \mu\bar{\mu}$ and the ε'/ε-anomaly will be fully established in the future, the VLQ models based on the SM gauge group would offer the best explanation among VLQ models. If, on the other hand, the B physics anomalies will be confirmed in the future and no visible NP will be found in rare K decays, VLQ models with $\mathrm{U}(1)_{L_\mu - L_\tau}$ would be favored.

Lesson 14: A large enhancement of $\mathcal{B}(K^+ \to \pi^+\nu\bar{\nu})$ would uniquely select RH VLQ models with a second doublet Φ subject to the future status of ΔM_K, although LH models with SM gauge group and the ones with $\mathrm{U}(1)_{L_\mu - L_\tau}$ and Φ could provide a moderate enhancement, in case of the latter depending on the theoretical treatment of $K_L \to \mu\bar{\mu}$. On the other hand, a large enhancement of $\mathcal{B}(B \to K^{(*)}\nu\bar{\nu})$ would disfavor all considered models, at least with only one VLQ representation. Some improvements are possible in the presence of several representations.

While the discovery of VLQs at the LHC would give a strong impetus to the models considered here, nonobservation of them at the LHC would not preclude their importance for flavor physics. In fact, as has been shown in [666], large NP effects in flavor observables can be present for $M_{\rm VLQ} = 10$ TeV, and in the flavor-precision era one is sensitive to even higher scales. In this context one finds that the combination of $|\Delta F| = 2$ and $|\Delta F| = 1$ observables in a given meson system generally allows to determine the masses of VLQs in a given representation independent of the size of Yukawa couplings.

Finally, those readers who got motivated to construct new UV completions with VLQs should first read [1033].

16.3.6 Vector-Like Leptons

According to the classification in [967] there are six renormalizable models with vector-like leptons (VLL) in a single complex representation of the SM gauge group. The literature on these models is not as rich as on VLQ and is dominated by the desire to explain the $(g-2)_\mu$ anomaly [943, 1034–1038]. For collider signatures see, e.g., [1039]. We can recommend also the analysis in [1040], where a model with a complete vector-like fourth family and additional $\mathrm{U}(1)'$ symmetry has been proposed. One can then see VLQs, VLLs, and Z' together in action with the goal to explain the $(g-2)_\mu$ anomaly and $b \to s\ell^+\ell^-$ anomalies in the context of a rich flavor structure. We hope to describe the physics of VLLs in the second edition of this book.

Downloaded from https://www.cambridge.org/core. UNIVERSIDAD AUTONOMA METROPOLITANA, on 16 Nov 2026 at 12:03:57, subject to the Cambridge Core terms of use, available at https://www.cambridge.org/core/terms. https://doi.org/10.1017/9781139524100.022

16.4 Leptoquark Models

16.4.1 Introduction

Leptoquarks (LQs) are very special new particles as they directly couple quarks to leptons and consequently carry both baryon and lepton number, B and L. Moreover, they are strongly interacting and carry fractional electric charges, but in contrast to quarks and leptons they are bosons: either scalars or vectors [1041–1044]. Because of these rather special properties of LQs the phenomenological implications of models containing them are markedly different from the ones where new scalars and gauge bosons couple directly only leptons to leptons and quarks to quarks. They also differ from those just discussed in VLQ models.

Indeed quite generally the pattern of flavor violations within LQ models is as follows.

- The semileptonic and leptonic decays of mesons are privileged as in these models they can naturally appear already at tree-level. This applies in particular to many rare decays which are loop suppressed within the SM. Therefore, the presence of departures from SM expectations for such decays can naturally be explained in some LQ models.
- On the other hand, all nonleptonic decays of mesons and also purely leptonic processes are loop-suppressed within LQ models.
- In consequence, large LQ effects in semileptonic and leptonic decays of mesons do not necessarily imply large modifications of SM predictions for nonleptonic observables for which the SM, with few notable exceptions like ε'/ε and $\Delta M_{d,s}$, offers a good description of the data. On the other hand, in view of a very strong suppression of FCNC in purely leptonic processes within the SM, still large LQ effects in these processes can be found despite their loop suppression providing thereby strong constraints on LQ models.
- Moreover, it should be emphasized that in LQ models in which the only new particles are LQs, the fermions exchanged in the loops are leptons in nonleptonic meson decays but SM quarks in the case of purely leptonic processes. Therefore Z-penguin diagrams that are important for several nonleptonic FCNC processes in the SM because of the large top-quark mass are very strongly suppressed in LQ models by the ratios of lepton masses and LQ masses. In consequence, in these models Z-penguin diagrams do not play any role in nonleptonic processes but can be important in purely leptonic processes in which quarks, in particular the top-quark, can be exchanged in the loop.
- Nonleptonic decays in LQ models are then expected at first sight to be governed by gluon-penguins rather than Z-penguins but these effects turn out to be subleading. Indeed, as pointed out in [667], in the context of ε'/ε the dominant contributions to this ratio originate from the electroweak effects in the renormalization group evolution between LQ scale and electroweak scale. This evolution generates through mixing four-quark operators contributing to ε'/ε from semileptonic operators, characteristic for LQ models. In addition in models with both left-handed and right-handed couplings enhanced box diagram contributions to ε'/ε are possible. However, as demonstrated in [667] and presented at the end of this section, when constraints from other processes

Downloaded from https://www.cambridge.org/core. UNIVERSIDAD AUTONOMA METROPOLITANA, on 16 Nov 2026 at 12:03:57, subject to the Cambridge Core terms of use, available at https://www.cambridge.org/core/terms. https://doi.org/10.1017/9781139524100.022

are taken into account, these effects are unlikely to be able to explain the ε'/ε-anomaly discussed in Section 10.5.

The suppression of LQ contributions to nonleptonic transitions in LQ models is certainly useful for those nonleptonic observables for which the SM predictions agree well with data, as strong constraints on LQ parameters from them can be avoided, making the explanation of B physics anomalies in semileptonic decays easier. On the other hand, as mentioned already in the context of ε'/ε, in cases in which the SM would have problems with explaining the data on nonleptonic decays and transitions, LQs are expected to be challenged because bringing the theory to agree with data will likely imply too large deviations in at least some tree-level mediated decays.

There is a very rich literature on LQs with extensive analyses of collider, electroweak, and flavor-violating processes among others. In particular, a model-independent Lagrangian of LQs that is invariant under the SM gauge group $\mathrm{SU}(3)_C \otimes \mathrm{SU}(2)_L \otimes \mathrm{U}(1)_Y$ and conserves B and L was given first in [1041] (see also [1042]). Extensive phenomenology based on this Lagrangian can be found in [1043]; however, many aspects were already discussed before throughout the literature. The analyses in [1045–1048] are particularly useful and informative. For reviews see [1044, 1049] and section 7 of [305].

The goal of the present section is to summarize the properties of leptoquarks, five scalar leptoquarks, and five vector leptoquarks. We give the transformation properties of them under the SM gauge group and present the model-independent, as far as Yukawa couplings are concerned, Lagrangian from which general flavor properties of the 10 leptoquarks can be deduced. In this context we allow leptoquarks to couple to all generations of ordinary quarks and leptons. Even if this increases the number of free parameters, it is useful to present the general formulas for various observables without any particular assumptions on Yukawa couplings. On the other hand, we will confine a detailed discussion of various observables to five models that were studied extensively in the literature. These are three scalar leptoquark models with leptoquarks transforming as doublets (R_2, $\tilde{R}_2$) and triplet (S_3) under the $\mathrm{SU}(2)_L$ and two vector leptoquark models with leptoquarks transforming as singlet (U_1) and a triplet (U_3) under $\mathrm{SU}(2)_L$. The interest in $\tilde{R}_2$, S_3, and U_3 models is that all three provide NP contributions to most interesting rare decays $K^+ \to \pi^+\nu\bar{\nu}$, $K_\mathrm{L} \to \pi^0\nu\bar{\nu}$, and $K_{L,S} \to \mu^+\mu^-$ and those governed by the transitions $b \to s\mu^+\mu^-$, $b \to s\nu\bar{\nu}$, and $b \to c\ell\nu$, in particular the decays $B_d \to D(D^*)\tau\nu_\tau$. As we have seen in previous sections, all these transitions are of great interest in view of new measurements to be performed in this decade and expected advances in the theory.

The remaining two models, R_2 and U_1, are special as in these models LQs do not contribute to $K_\mathrm{L} \to \pi^0\nu\bar{\nu}$, $K^+ \to \pi^+\nu\bar{\nu}$, and $b \to s\nu\bar{\nu}$ transitions at tree-level. Even if RG effects generate such transitions and they can be generated through one-loop matching, this feature allows to face easier the constraints from decays with $\nu\bar{\nu}$ in the final state than it is possible in other models.

Having explicit formulas at hand will allow us to have another look at the anomalies observed in the $b \to s\mu^+\mu^-$ transitions but this time in LQ models. $K^+ \to \pi^+\nu\bar{\nu}$ and $K_\mathrm{L} \to \pi^0\nu\bar{\nu}$ are of great interest in view of new measurements of their branching ratios by NA62 and KOPIO and $b \to s\nu\bar{\nu}$ transitions in view of Belle II experiments. NP in

Downloaded from https://www.cambridge.org/core. UNIVERSIDAD AUTONOMA METROPOLITANA, on 16 Nov 2026 at 12:03:57, subject to the Cambridge Core terms of use, available at https://www.cambridge.org/core/terms. https://doi.org/10.1017/9781139524100.022

these models enters also $\Delta F = 2$ transitions and the ratio ε'/ε. Moreover, in some of these observables departures from SM expectations have been found, and in fact an increased interest in LQs arose from the fact that some of these anomalies could be attributed to these new particles.

We will only briefly discuss the remaining models and hybrid scenarios in which two or more leptoquarks in different representations are present exhibiting new features relative to the five models listed earlier. An important issue in LQ models is the proton decay that in some models takes place already at tree-level excluding such models for LQ masses of $O(1\,\text{TeV})$ unless some discrete symmetries are imposed.

The material presented in this section originated in an extensive collaboration with Christoph Bobeth, which includes not only the aspects related to [667] but also beyond it.

16.4.2 Model-Independent Leptoquark Lagrangian

Quantum Numbers and the Basic Lagrangian

The LQs are singlets, doublets, or triplets w.r.t. to $\text{SU}(2)_L$. There quantum numbers and transformation properties under the SM gauge group are collected in Table 16.4 with our convention

$$Q = T_3 + Y. \tag{16.65}$$

The superscript $i = (1, 2, 3)$ corresponds to the $\text{SU}(2)_L$ multiplet (singlet, doublet, triplet) to which the LQs belong. All color-antitriplets (S_1, $\tilde{S}_1$, S_3, V_2, $\tilde{V}_2$) carry fermion number

$$F = 3B + L = -2, \tag{16.66}$$

whereas all color-triplets (U_1, $\tilde{U}_1$, U_3, R_2, $\tilde{R}_2$) carry $F = 0$.

The phenomenological LQ Lagrangian that describes the interactions of spin-0 (S) and spin-1 (V) LQs with quarks and leptons is given as follows

$$\mathcal{L}_{\text{LQ}} = \mathcal{L}_S + \mathcal{L}_V + \text{h.c.}, \tag{16.67}$$

where adopting the conventions from [1050] we have

$$\begin{aligned}\mathcal{L}_S = &\left(g^{1L}\left[\overline{Q_L^c} i\sigma_2 L_L\right] + g^{1R}\left[\overline{u_R^c}\ell_R\right]\right) S_1 + \tilde{g}^{1R}\left[\overline{d_R^c}\ell_R\right]\tilde{S}_1 \\ &+ h^{2L}\left[\overline{u_R} R_2^T i\sigma_2 L_L\right] + h^{2R}\left[\overline{Q_L} R_2 \ell_R\right] + \tilde{h}^{2L}\left[\overline{d_R}\tilde{R}_2^T i\sigma_2 L_L\right] \\ &+ g^{3L}\left[\overline{Q_L^c} i\sigma_2 \vec{\tau} L_L\right]\cdot\vec{S}_3,\end{aligned} \tag{16.68}$$

$$\begin{aligned}\mathcal{L}_V = &\left(h^{1L}\left[\overline{Q_L}\gamma_\mu L_L\right] + h^{1R}\left[\overline{d_R}\gamma_\mu \ell_R\right]\right) U_1^\mu + \tilde{h}^{1R}\left[\overline{u_R}\gamma_\mu\ell_R\right]\tilde{U}_1^\mu \\ &+ g^{2L}\left[\overline{d_R^c}\gamma_\mu (V_2^\mu)^T i\sigma_2 L_L\right] + g^{2R}\left[\overline{Q_L^c}\gamma_\mu i\sigma_2 V_2^\mu \ell_R\right] + \tilde{g}^{2L}\left[\overline{u_R^c}\gamma_\mu(\tilde{V}_2^\mu)^T i\sigma_2 L_L\right] \\ &+ h^{3L}\left[\overline{Q_L}\gamma_\mu\vec{\tau} L_L\right]\cdot\vec{U}_3^\mu\,.\end{aligned} \tag{16.69}$$

Downloaded from https://www.cambridge.org/core. UNIVERSIDAD AUTONOMA METROPOLITANA, on 16 Nov 2026 at 12:03:57, subject to the Cambridge Core terms of use, available at https://www.cambridge.org/core/terms. https://doi.org/10.1017/9781139524100.022

Table 16.4 Quantum numbers of interactions of LQs.[a]

LQ	$SU(3)_c$	$SU(2)_L$	$U(1)_Y$	T_3	Q_{em}	$d_i, \ell^+\ell^-$	$d_i, \nu\bar{\nu}$	$u_i, \ell^+\ell^-$	$u_i, \nu\bar{\nu}$
S_1	3^*	1	1/3	0	1/3		*	*	
$\tilde{S}_1$	3^*	1	4/3	0	4/3	*			
R_2	3	2	7/6	+1/2	5/3			*	
				−1/2	2/3	*			*
$\tilde{R}_2$	3	2	1/6	+1/2	2/3	*			
				−1/2	−1/3		*		
S_3	3^*	3	1/3	+1	4/3	*			
				0	1/3		*	*	
				−1	−2/3				*
U_1	3	1	2/3	0	2/3	*			*
$\tilde{U}_1$	3	1	5/3	0	5/3			*	
V_2	3^*	2	5/6	+1/2	4/3	*			
				−1/2	1/3		*	*	
$\tilde{V}_2$	3^*	2	−1/6	+1/2	1/3			*	
				−1/2	−2/3				*
U_3	3	3	2/3	+1	5/3			*	
				0	2/3	*			*
				−1	−1/3		*		

[a] The stars indicate to which procesess a given LQ contributes to at tree-level. Note that antitriplets 3^* interact with charge conjugated quark fields.

The $A = (L, R)$-superscript in the couplings y^{iA} ($y = g, \tilde{g}, h, \tilde{h}$) indicates the chirality of the leptons in the coupling, and σ_i are Pauli matrices given again in (16.86). The $\vec{\tau}$, relevant for triplet representations, are defined in (16.87). Q^c, u^c, d^c are charge-conjugated fields.

The fermion fields are the usual quark and lepton left-handed $SU(2)_L$ doublets Q_L and L_L as well as the right-handed singlets u_R, d_R, and ℓ_R. For convenience we recall their hypercharges

$$Y(Q_L) = +1/6, \quad Y(L_L) = -1/2, \quad Y(u_R) = +2/3, \quad Y(d_R) = -1/3, \quad Y(\ell_R) = -1. \tag{16.70}$$

If ν_R is included additional terms appear in the Lagrangians [1042].

We will now expand the $SU(2)_L$ structure to make explicit the interactions of up- and down-type quarks and leptons with $SU(2)_L$ components of the LQ fields. For this purpose, we denote components of the LQ doublet $X_2 = (R_2, \tilde{R}_2, V_2, \tilde{V}_2)$ and triplet $X_3 = (S_3, U_3)$ fields as

$$(X_2)_a = X_{2,a}, \qquad a = (+, -), \tag{16.71}$$

$$(X_3)_a = X_{3,a}, \qquad a = (1, 2, 3). \tag{16.72}$$

Downloaded from https://www.cambridge.org/core. UNIVERSIDAD AUTONOMA METROPOLITANA, on 16 Nov 2026 at 12:03:57, subject to the Cambridge Core terms of use, available at https://www.cambridge.org/core/terms. https://doi.org/10.1017/9781139524100.022

Note that the triplet fields correspond to a Cartesian representation with complex fields $X_{3,a}$. To have a representation where the components correspond to a definite isospin, one has to transform the fields to the spherical basis $Y_{3,i}$:

$$Y_{3,\pm} = \frac{1}{\sqrt{2}}(X_{3,1} \mp iX_{3,2}), \qquad Y_{3,0} = X_{3,3}, \tag{16.73}$$

where $i = (+, 0, -)$ denotes isospin $(+1, 0, -1)$ for $Y_{3,i}$. The Cartesian and spherical bases are related via the unitary transformation

$$Y = U^\dagger X, \qquad U = \frac{1}{\sqrt{2}}\begin{pmatrix} 1 & 0 & 1 \\ i & 0 & -i \\ 0 & \sqrt{2} & 0 \end{pmatrix}. \tag{16.74}$$

Lagrangian in SU(2)$_L$ Components

Rewriting the Lagrangian in (16.68) in terms of SU(2)$_L$ components we find

$$\begin{aligned}\mathcal{L}_{S_1} = &\left\{ g^{1L} \quad \left([\overline{u^c} P_L \ell] - [\overline{d^c} P_L \nu]\right) + \; g^{1R} \quad [\overline{u^c} P_R \ell]\right\} S_1 \\ &+ \left\{(g^{1L})^\dagger \left([\bar{\ell} P_R u^c] - [\bar{\nu} P_R d^c]\right) + (g^{1R})^\dagger [\bar{\ell} P_L u^c]\right\} S_1^*,\end{aligned} \tag{16.75}$$

$$\mathcal{L}_{\tilde{S}_1} = \tilde{g}^{1R} [\overline{d^c} P_R \ell] \tilde{S}_1 + (\tilde{g}^{1R})^\dagger [\bar{\ell} P_L d^c] \tilde{S}_1^*, \tag{16.76}$$

$$\begin{aligned}\mathcal{L}_{R_2} = \; & h^{2L} \quad ([\bar{u} P_L \ell] R_{2,+} - [\bar{u} P_L \nu] R_{2,-}) + \; h^{2R} \quad \left([\bar{u} P_R \ell] R_{2,+} + [\bar{d} P_R \ell] R_{2,-}\right) \\ &+ (h^{2L})^\dagger \left([\bar{\ell} P_R u] R_{2,+}^* - [\bar{\nu} P_R u] R_{2,-}^*\right) + (h^{2R})^\dagger \left([\bar{\ell} P_L u] R_{2,+}^* + [\bar{\ell} P_L d] R_{2,-}^*\right),\end{aligned} \tag{16.77}$$

$$\mathcal{L}_{\tilde{R}_2} = \tilde{h}^{2L} \left([\bar{d} P_L \ell] \tilde{R}_{2,+} - [\bar{d} P_L \nu] \tilde{R}_{2,-}\right) + (\tilde{h}^{2L})^\dagger \left([\bar{\ell} P_R d] \tilde{R}_{2,+}^* - [\bar{\nu} P_R d] \tilde{R}_{2,-}^*\right), \tag{16.78}$$

$$\begin{aligned}\mathcal{L}_{S_3} = \; & g^{3L} \quad \left[\sqrt{2}\,[\overline{u^c} P_L \nu] S_{3,-} - \sqrt{2}\,[\overline{d^c} P_L \ell] S_{3,+} - (\overline{u^c} P_L \ell + \overline{d^c} P_L \nu) S_{3,0}\right] \\ &+ (g^{3L})^\dagger \left[\sqrt{2}\,[\bar{\nu} P_R u^c] S_{3,-}^* - \sqrt{2}\,[\bar{\ell} P_R d^c] S_{3,+}^* - (\bar{\ell} P_R u^c + \bar{\nu} P_R d^c) S_{3,0}^*\right].\end{aligned} \tag{16.79}$$

For the vector leptoquarks we obtain from (16.69)

$$\begin{aligned}\mathcal{L}_{U_1} = &\left\{ h^{1L} \quad \left([\bar{u} \gamma_\mu P_L \nu] + [\bar{d} \gamma_\mu P_L \ell]\right) + \; h^{1R} \quad [\bar{d} \gamma_\mu P_R \ell]\right\} U_1^\mu \\ &+ \left\{(h^{1L})^\dagger \left([\bar{\nu} \gamma_\mu P_L u] + [\bar{\ell} \gamma_\mu P_L d]\right) + (h^{1R})^\dagger [\bar{\ell} \gamma_\mu P_R d]\right\} U_1^{\mu,*},\end{aligned} \tag{16.80}$$

Downloaded from https://www.cambridge.org/core. UNIVERSIDAD AUTONOMA METROPOLITANA, on 16 Nov 2026 at 12:03:57, subject to the Cambridge Core terms of use, available at https://www.cambridge.org/core/terms. https://doi.org/10.1017/9781139524100.022

$$\mathcal{L}_{\tilde{U}_1} = \tilde{h}^{1R}[\bar{u}\gamma_\mu P_R \ell]\tilde{U}_1^\mu + (\tilde{h}^{1R})^\dagger[\bar{\ell}\gamma_\mu P_R u]\tilde{U}_1^{\mu,*}, \tag{16.81}$$

$$\begin{aligned}\mathcal{L}_{V_2} = {} & g^{2L}\left([\overline{d^c}\gamma_\mu P_L \ell]V_{2,+}^\mu - [\overline{d^c}\gamma_\mu P_L \nu]V_{2,-}^\mu\right) + g^{2R}\left([\overline{u^c}\gamma_\mu P_R \ell]V_{2,-}^\mu - [\overline{d^c}\gamma_\mu P_R \ell]V_{2,+}^\mu\right) \\ & + (g^{2L})^\dagger\left([\bar{\ell}\gamma_\mu P_L d^c]V_{2,+}^{\mu,*} - [\bar{\nu}\gamma_\mu P_L d^c]V_{2,-}^{\mu,*}\right) + (g^{2R})^\dagger\left([\bar{\ell}\gamma_\mu P_R u^c]V_{2,-}^{\mu,*} - [\bar{\ell}\gamma_\mu P_R d^c]V_{2,+}^{\mu,*}\right),\end{aligned} \tag{16.82}$$

$$\mathcal{L}_{\tilde{V}_2} = \tilde{g}^{2L}\left([\overline{u^c}\gamma_\mu P_L \ell]\tilde{V}_{2,+}^\mu - [\overline{u^c}\gamma_\mu P_L \nu]\tilde{V}_{2,-}^\mu\right) + (\tilde{g}^{2L})^\dagger\left([\bar{\ell}\gamma_\mu P_L u^c]\tilde{V}_{2,+}^{\mu,*} - [\bar{\nu}\gamma_\mu P_L u^c]\tilde{V}_{2,-}^{\mu,*}\right), \tag{16.83}$$

$$\begin{aligned}\mathcal{L}_{U_3} = {} & h^{3L}\left[\sqrt{2}\,[\bar{u}\gamma_\mu P_L \ell]U_{3,+}^\mu + \sqrt{2}\,[\bar{d}\gamma_\mu P_L \nu]U_{3,-}^\mu + (\bar{u}\gamma_\mu P_L \nu - \bar{d}\gamma_\mu P_L \ell)U_{3,0}^\mu\right] \\ & + (h^{3L})^\dagger\left[\sqrt{2}\,[\bar{\ell}\gamma_\mu P_L u]U_{3,+}^{\mu,*} + \sqrt{2}\,[\bar{\nu}\gamma_\mu P_L d]U_{3,-}^{\mu,*} + (\bar{\nu}\gamma_\mu P_L u - \bar{\ell}\gamma_\mu P_L d)U_{3,0}^{\mu,*}\right].\end{aligned} \tag{16.84}$$

We summarize all interactions in Table 16.4. Their impact on flavor observables in the case of R_2, $\tilde{R}_2$, S_3, U_1, and U_3 models will be worked out in Section 16.4.4. General properties of the remaining models will be summarized at the end of this section.

It should be emphasized that the preceding formulas are in the flavor eigenbasis of quarks and leptons, and rotations to the mass eigenbasis have to be performed, depending on the mass generation mechanism of quarks and leptons, i.e., for example, in the SM from diagonalization of Yukawa couplings with one Higgs doublet and via SSB – bringing in potential factors from the CKM and PMNS matrices. See, for example, eqs. (2.2) and (2.6) in [1046]. This issue has been already discussed in the context of vector-like quarks with explicit formulas given in (16.36) and (16.37). As there, we will take the freedom to choose the weak basis such that down-type quarks are already mass eigenstates, which fixes $V_{L,R}^d = \mathbb{1}$, and assume without loss of generality $V_R^u = \mathbb{1}$, yielding $q_L = (V^\dagger u_L, d_L)^T$. Analogously, we choose also the down-type lepton mass matrix to be diagonal and leave the neutrinos in the flavor eigenbasis. This defines the SMEFT Wilson coefficients below the LQ scale unambiguously and avoids the appearance of the PMNS lepton-mixing matrix in interactions involving neutrinos.

LQ Kinetic and Gauge Interactions

The kinetic and gauge interactions for a LQ Φ are fixed from the quantum numbers given in Table 16.4. The covariant derivative under $\mathrm{SU}(2)_L \otimes \mathrm{U}(1)_Y$ for the components Φ_α of a LQ multiplet under $\mathrm{SU}(2)_L$ is given by

$$D_\mu \Phi_\alpha = \left[\partial_\mu \delta_{\alpha\beta} - i g_2 \tau^a_{\alpha\beta} W^a_\mu - i g_1 Y_\Phi \delta_{\alpha\beta} B_\mu\right]\Phi_\beta, \tag{16.85}$$

where the $\mathrm{SU}(2)_L$ generators τ^a depend on the representation of Φ under $\mathrm{SU}(2)_L$. For doublets $\tau^a = \sigma_a/2$ is given by the Pauli matrices

$$\sigma_1 = \begin{pmatrix} 0 & 1 \\ 1 & 0 \end{pmatrix}, \qquad \sigma_2 = \begin{pmatrix} 0 & -i \\ i & 0 \end{pmatrix}, \qquad \sigma_3 = \begin{pmatrix} 1 & 0 \\ 0 & -1 \end{pmatrix}. \tag{16.86}$$

Downloaded from https://www.cambridge.org/core. UNIVERSIDAD AUTONOMA METROPOLITANA, on 16 Nov 2026 at 12:03:57, subject to the Cambridge Core terms of use, available at https://www.cambridge.org/core/terms. https://doi.org/10.1017/9781139524100.022

For triplets in the spherical representation Y in (16.73) one has $\tau^a = t^a$ with t^a being the generators of $\mathrm{SU}(2)_L$ given in the adjoint representation as follows

$$t^1 = \frac{1}{\sqrt{2}}\begin{pmatrix} 0 & -1 & 0 \\ -1 & 0 & 1 \\ 0 & 1 & 0 \end{pmatrix}, \qquad t^2 = \frac{1}{\sqrt{2}}\begin{pmatrix} 0 & i & 0 \\ -i & 0 & -i \\ 0 & i & 0 \end{pmatrix}, \qquad t^3 = \begin{pmatrix} 1 & 0 & 0 \\ 0 & 0 & 0 \\ 0 & 0 & -1 \end{pmatrix}. \tag{16.87}$$

The diagonalization of the $\mathrm{SU}(2)_L \otimes \mathrm{U}(1)_Y$ gauge sector is the usual one of the SM, but we repeat it here for convenience. We have

$$\sqrt{2}W^{\pm}_\mu = W^1_\mu \mp i W^2_\mu, \qquad A_\mu = c_W B_\mu + s_W W^3_\mu, \qquad Z_\mu = -s_W B_\mu + c_W W^3_\mu. \tag{16.88}$$

The weak mixing angle ϑ_W and the $\mathrm{U}(1)_{\mathrm{em}}$ coupling are related to $g_{1,2}$ as

$$s_W \equiv \sin(\vartheta_W) = \frac{g_1}{\sqrt{g_1^2 + g_2^2}}, \qquad c_W \equiv \cos(\vartheta_W) = \frac{g_2}{\sqrt{g_1^2 + g_2^2}}, \qquad e = \frac{g_1 g_2}{\sqrt{g_1^2 + g_2^2}}. \tag{16.89}$$

Moreover, with the vacuum expectation value $v = \sqrt{\mu^2/\lambda} = 246\,\mathrm{GeV}$ one has

$$M_W = \frac{g_2}{2}v, \qquad M_Z = \frac{\sqrt{g_1^2 + g_2^2}}{2}v, \qquad e = g_1 c_W = g_2 s_W, \qquad M_W = c_W M_Z. \tag{16.90}$$

The covariant derivative (16.85) will be then

$$D_\mu = \partial_\mu - i\frac{g_2}{\sqrt{2}}\left(\tau^+ W^+_\mu + \tau^- W^-_\mu\right) - i\frac{g_2}{c_W}(\tau^3 - s_W^2 Q)\, Z_\mu - ieQ\, A_\mu. \tag{16.91}$$

Here

$$\tau^\pm = \tau^1 \pm i\tau^2, \qquad Q = Y\mathbb{1} + \tau^3. \tag{16.92}$$

The corresponding expression for $\mathrm{SU}(2)_L$-singlet LQs is easily obtained by omitting terms with $\tau^{+,-,3}$. For doublets

$$\tau^+ = \begin{pmatrix} 0 & 1 \\ 0 & 0 \end{pmatrix}, \qquad \tau^- = \begin{pmatrix} 0 & 0 \\ 1 & 0 \end{pmatrix}, \qquad \tau^3 = \frac{1}{2}\begin{pmatrix} 1 & 0 \\ 0 & -1 \end{pmatrix}, \tag{16.93}$$

and for triplets using (16.87)

$$\tau^+ = \frac{2}{\sqrt{2}}\begin{pmatrix} 0 & -1 & 0 \\ 0 & 0 & 1 \\ 0 & 0 & 0 \end{pmatrix}, \qquad \tau^- = \frac{2}{\sqrt{2}}\begin{pmatrix} 0 & 0 & 0 \\ -1 & 0 & 0 \\ 0 & 1 & 0 \end{pmatrix}, \qquad \tau^3 = \begin{pmatrix} 1 & 0 & 0 \\ 0 & 0 & 0 \\ 0 & 0 & -1 \end{pmatrix}. \tag{16.94}$$

The kinetic and gauge terms are given by

$$\mathcal{L}_{\mathrm{kin}} = (D_\mu \Phi)^\dagger (D^\mu \Phi) + \text{LQ mass term} \tag{16.95}$$

using (16.91).

Downloaded from https://www.cambridge.org/core. UNIVERSIDAD AUTONOMA METROPOLITANA, on 16 Nov 2026 at 12:03:57, subject to the Cambridge Core terms of use, available at https://www.cambridge.org/core/terms. https://doi.org/10.1017/9781139524100.022

Additional interactions of LQs with the SM Higgs doublet were introduced in [1051]. In consequence the LQs of different $SU(2)_L$ multiplets start to mix and phenomenology becomes more involved. See, for example, the generation of tensor operators for $b \to s\bar{\ell}\ell$ [487, 1045].

16.4.3 Selection of Models

It should be stressed that until now we did not specify the structure of Yukawa couplings, which even within one of these 10 scenarios for LQs contains a large model dependence unless some fundamental theory predicting or constraining these couplings has been constructed. One should remember that these Yukawa couplings y^{iA} are general complex 3×3 matrices, and this introduces many free parameters. Moreover, within a given theory, there could be several generations of LQs having the same transformation properties under $SU(2)_L$. Consequently, one could construct several models depending on which of this situations is realized. Some of the obvious possibilities are

1. The couplings y^{iA} are diagonal in generation space of quarks and leptons, and there are several generations for each LQ representation.
2. The couplings y^{iA} are general 3×3 matrices in generation space, and there is just one LQ.
3. Or a combined version of the two aforementioned variants, i.e., the couplings y^{iA} are general 3×3 matrices in generation space that carry also a generation index for several generations of LQs. That is, every leptoquark has its own 3×3 Yukawa coupling.
4. Several LQ representations are considered simultaneously.

Most phenomenological studies found in the literature are restricted to one generation of LQs with general 3×3 couplings y^{iA} in the generation space. But also models with different LQ representations have been considered with the goal to avoid some experimental constraints. See, e.g., [719, 1052, 1053].

Here, to reduce the numbers of free parameters we will first consider models in which

- Only one LQ representation is present.
- Only one generation of LQs is present, which means that we have to deal in most models with one Yukawa coupling describing either left-handed or right-handed interactions. But in models S_1, R_2, U_1, and V_2 both interactions (without taking h.c. in scalar models) can be present. Only R_2 and U_1 will be discussed in some detail here.
- A given LQ couples to both charged leptons and neutrinos as this increases the number of constraints and makes our analysis more interesting.

The inspection of Table 16.4 shows that this selects the first three models among the five models, which we will discuss in some detail first,

$$S_3, \qquad U_3, \qquad \tilde{R}_2, \qquad U_1, \qquad R_2, \tag{16.96}$$

and these three models will be analyzed by us in some detail first. U_1 and R_2 LQs do not couple to neutrinos at tree-level, which presently is an advantage over the other three models as it allows to avoid constraints from $b \to s\nu\bar{\nu}$ processes. As R_2, $\tilde{R}_2$, and S_3 involve

Downloaded from https://www.cambridge.org/core. UNIVERSIDAD AUTONOMA METROPOLITANA, on 16 Nov 2026 at 12:03:57, subject to the Cambridge Core terms of use, available at https://www.cambridge.org/core/terms. https://doi.org/10.1017/9781139524100.022

scalar LQs and U_1 and U_3 vector LQs, we will also see explicitly the differences arising from the different spins of these particles. But the problem is that U_1 and U_3 models as they stand are non-renormalizable, and we will only be able to present the results from tree-level diagrams and leading RG effects for which no loops with internal LQs have to be evaluated. This situation can be improved by providing ultraviolet (UV) completion for these models. On the other hand, we will be able to do loop calculations for scalar LQs.

16.4.4 General Structure of Basic Formulas

It will be useful to use the technology of previous chapter and calculate the impact of LQs on various processes as shifts in the master functions known from CMFV models. Similar to models with Z' tree-level FCNC and VLQ models discussed in the previous section, also in the case of LQ models flavor universality of master functions is broken, and they depend on the meson considered. Moreover, they become complex quantities bringing new CP-violating effects. The use of this technology will facilitate the comparison with other models and will avoid the repetition of the formulas for observables in which the master functions listed here should be inserted. For our purposes it will be sufficient to consider the following functions, which we recall here for convenience.

For $\Delta F = 2$ transitions we have

$$S(K), \qquad S(B_d), \qquad S(B_s), \tag{16.97}$$

which describe among others ε_K, ΔM_d, and ΔM_s, respectively. The latter two allow to calculate NP effects in the CP-asymmetries $S_{\psi K_S}$ and $S_{\psi\phi}$. For decays with $\mu\bar{\mu}$ in the final state we have

$$Y_{\rm A}(K), \qquad Y_{\rm A}(B_d), \qquad Y_{\rm A}(B_s) \tag{16.98}$$

and for decays with $\nu\bar{\nu}$ in the final state

$$X(K), \qquad X(B_d), \qquad X(B_s). \tag{16.99}$$

In this particular case, when distinguishing between different neutrinos, we will have to generalize these functions to X^{ij} with the indices denoting different neutrinos.

The relevant CKM factors are again

$$\lambda_i^{(K)} = V_{is}^* V_{id}, \qquad \lambda_t^{(d)} = V_{tb}^* V_{td}, \qquad \lambda_t^{(s)} = V_{tb}^* V_{ts}, \tag{16.100}$$

and

$$g_{\rm SM}^2 = 4\frac{M_W^2 G_F^2}{2\pi^2} = 1.78137 \times 10^{-7}\,{\rm GeV}^{-2}. \tag{16.101}$$

This allows to introduce for each LQ the dimensionless quantity

$$\boxed{\kappa({\rm LQ}) = \frac{1}{g_{\rm SM}^2 m_{\rm LQ}^2} = 1.403, \qquad (m_{\rm LQ} = 2\,{\rm TeV}),} \tag{16.102}$$

which makes the following formulas more transparent.

Downloaded from https://www.cambridge.org/core. UNIVERSIDAD AUTONOMA METROPOLITANA, on 16 Nov 2026 at 12:03:57, subject to the Cambridge Core terms of use, available at https://www.cambridge.org/core/terms. https://doi.org/10.1017/9781139524100.022

In the case of the shifts ΔS it is useful to introduce the notation for sums of products of LQ couplings ($q = d, s$)

$$\boxed{Y^i_{Qq} \equiv \sum_a y^i_{Qa}\ (y^i_{qa})^*,} \tag{16.103}$$

where y stands for all the LQ couplings g, $\tilde{g}$, h, $\tilde{h}$ in (16.68) and (16.69), and Y are accordingly for G, $\tilde{G}$, H, $\tilde{H}$, with $i = 1L, 1R, 2L, 2R, 3L$. The summation is either over the neutrinos or charged leptons, which are exchanged in the box diagrams together with LQs. In the case of models considered next, and as explained earlier, working with down-quarks and charged leptons without any rotations from flavor basis and choosing the flavor basis for neutrinos, these sums are the same for neutrinos and charged leptons. We will therefore encounter only

$$\boxed{G^{3L}_{Qq} = \sum_a g^{3L}_{Qa}\ \left(g^{3L}_{qa}\right)^*, \qquad H^{3L}_{Qq} = \sum_a h^{3L}_{Qa}\ \left(h^{3L}_{qa}\right)^*, \qquad \tilde{H}^{2L}_{Qq} = \sum_a \tilde{h}^{2L}_{Qa}\ \left(\tilde{h}^{2L}_{qa}\right)^*,} \tag{16.104}$$

for S_3, U_3 and $\tilde{R}_2$, respectively. But the difference between neutrino and charged lepton contributions will be indicated in the following formulas through the masses of different LQs coupling to them.

On the other hand, in the U_1 model we will encounter

$$\boxed{H^{1L}_{Qq} = \sum_a h^{1L}_{Qa}\ \left(h^{1L}_{qa}\right)^*, \qquad H^{1R}_{Qq} = \sum_a h^{1R}_{Qa}\ \left(h^{1R}_{qa}\right)^*,} \tag{16.105}$$

and for R_2

$$\boxed{H^{2L}_{Qq} = \sum_a h^{2L}_{Qa}\ \left(h^{2L}_{qa}\right)^*, \qquad H^{2R}_{Qq} = \sum_a h^{2R}_{Qa}\ \left(h^{2R}_{qa}\right)^*.} \tag{16.106}$$

We will just quote the results as except for box diagrams the calculations are tree-level ones and very easy. In quoting the results for box diagrams we take into account that the masses of LQs are much larger than those of leptons so that lepton masses can be set to zero when evaluating these diagrams. The result for a box diagram is just a constant multiplied by some couplings. As there is no GIM mechanism in LQ models this constant remains at the end of the calculation. We advise motivated readers to check the following results. It is easier than many other calculations in this book.

Yet, a few comments should be made. While box diagram calculations result directly in the operators we encountered already in this book, tree diagrams of the type shown in Figure 16.2 result in operators like

$$(\bar{d}^i\gamma_\mu P_L l^j)(\bar{l}^l\gamma^\mu P_L d^k), \qquad (\bar{d}^i\gamma_\mu P_R l^j)(\bar{l}^l\gamma^\mu P_R d^k), \qquad (\bar{d}^i\gamma_\mu P_L l^j)(\bar{l}^l\gamma^\mu P_R d^k). \tag{16.107}$$

Downloaded from https://www.cambridge.org/core. UNIVERSIDAD AUTONOMA METROPOLITANA, on 16 Nov 2026 at 12:03:57, subject to the Cambridge Core terms of use, available at https://www.cambridge.org/core/terms. https://doi.org/10.1017/9781139524100.022

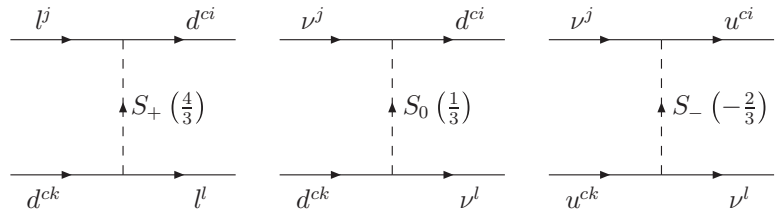


Figure 16.1 Tree-level contributions of S_+, S_0, and S_- in the S_3 model.

To find the Wilson coefficients of the operators consisting of product of quark and lepton currents, as encountered in this book, Fierz transformations have to be performed. One finds then, respectively,

$$(\bar{d}^i \gamma_\mu P_L d^k)(\bar{l}^l \gamma^\mu P_L l^j), \qquad (\bar{d}^i \gamma_\mu P_R d^k)(\bar{l}^l \gamma^\mu P_R l^j), \qquad -2(\bar{d}^i P_R d^k)(\bar{l}^l P_L l^j). \tag{16.108}$$

This means that in the presence of both LH and RH vector couplings, in LQ models scalar-scalar operators contribute to various observables. On the other hand in some models, like S_3, operators with LH and RH scalar couplings and charge conjugated fields, shown in Figure 16.1, are present. The corresponding Fierz transformations, which can be found in Appendix A.3, imply LR vector-vector operators. In case of the difficulties with charge conjugated fields the help comes from [1054].

Before entering the details, another important comment should be made. When listing the following results, we did not include any renormalization group effects that were discussed generally in Chapter 14. As the scales involving LQs are much higher than the EW scale, the shifts in the master functions listed following must be corrected by including these effects along the lines discussed in Chapter 14. Then it turns out that the results listed here do not necessarily dominate a given process because RG effects enhanced by large logarithms could be more important. This is, for instance, the case of LQ contributions to ε'/ε as analyzed in [667] and summarized in Section 16.4.13.

Finally, in the case of difficulties, the following formulas can be derived from the general SMEFT formulas, like the ones in (14.79), and the expressions for SMEFT coefficients in terms of LQ couplings and masses given in Appendix B of [667]. But to find the NP shifts in the usual WCs like C_9 and C_{10}, one has to remember to multiply the SMEFT coefficients in the latter paper and the ones in (14.79) by

$$\frac{\pi}{\alpha_e}\frac{v^2}{\lambda_t^{ji}} = \frac{1}{g_{\rm SM}^2 \sin^2\vartheta_W}\frac{1}{\lambda_t^{ji}} \tag{16.109}$$

as explicitly stated in (14.77).

After these introductory comments we are ready to list results for the chosen LQ models.

16.4.5 S_3

For the shifts ΔS we find

$$\Delta S(K) = \frac{\tilde{r}}{16\pi^2}\left[\frac{G_{sd}^{3L}}{\lambda_t^{(K)}}\right]^2 [4\,\kappa(S_+) + \kappa(S_0)] \tag{16.110}$$

Downloaded from https://www.cambridge.org/core. UNIVERSIDAD AUTONOMA METROPOLITANA, on 16 Nov 2026 at 12:03:57, subject to the Cambridge Core terms of use, available at https://www.cambridge.org/core/terms. https://doi.org/10.1017/9781139524100.022

and

$$\Delta S(B_q) = \frac{\tilde{r}}{16\pi^2}\left[\frac{G_{bq}^{3L}}{\lambda_t^{(q)}}\right]^2 [4\,\kappa(S_+) + \kappa(S_0)]\,, \tag{16.111}$$

where $\tilde{r} \approx 1$ is a QCD correction that takes into account RG effects between $\mu = m_{\rm LQ}$ and $\mu = m_t$ with the latter used as matching scale in the SM. The contributions of S_+ and S_0 involve charged leptons and neutrinos, respectively.

Calculating the first diagram in Figure 16.1, we find first

$$Y_A(K) = Y_{\rm SM} + \kappa(S_+)\left[\frac{g_{s\mu}^{3L}(g_{d\mu}^{3L})^*}{\lambda_t^{(K)}}\right], \qquad Y_A(B_q) = Y_{\rm SM} + \kappa(S_+)\left[\frac{g_{q\mu}^{3L}(g_{b\mu}^{3L})^*}{\lambda_t^{(q)}}\right]. \tag{16.112}$$

The same diagram implies also NP contributions to the Wilson coefficients C_9 and through Y_A to C_{10} giving

$$C_9^{\rm NP} = \frac{\kappa(S_+)}{\sin^2\vartheta_W}\left[\frac{g_{s\mu}^{3L}(g_{b\mu}^{3L})^*}{\lambda_t^{(s)}}\right], \qquad C_{10}^{\rm NP} = -C_9^{\rm NP}. \tag{16.113}$$

The relevant functions X^{ij} are found from the second diagram in Figure 16.1:

$$X^{ij}(K) = X_{\rm SM}\delta_{ij} - \frac{\kappa(S_0)}{2}\left[\frac{g_{sv_i}^{3L}(g_{dv_j}^{3L})^*}{\lambda_t^{(K)}}\right] \tag{16.114}$$

and

$$X^{ij}(B_q) = X_{\rm SM}\delta_{ij} - \frac{\kappa(S_0)}{2}\left[\frac{g_{qv_i}^{3L}(g_{bv_j}^{3L})^*}{\lambda_t^{(q)}}\right]. \tag{16.115}$$

Defining then

$$X_{\rm eff}^{ij} = \lambda_t^{(K)} X^{ij}(K) \tag{16.116}$$

the usual expressions for the branching ratios for $K^+ \to \pi^+\nu\bar{\nu}$ and $K_{\rm L} \to \pi^0\nu\bar{\nu}$ are generalized as follows

$$\mathcal{B}(K^+ \to \pi^+\nu\bar{\nu}) = \frac{\kappa_+}{3}\sum_{i,j}\left[\left(\frac{{\rm Im}\,X_{\rm eff}^{ij}}{\lambda^5}\right)^2 + \left(\frac{{\rm Re}\,\lambda_c}{\lambda}P_c(X)\delta_{ij} + \frac{{\rm Re}\,X_{\rm eff}^{ij}}{\lambda^5}\right)^2\right], \tag{16.117}$$

$$\mathcal{B}(K_{\rm L} \to \pi^0\nu\bar{\nu}) = \frac{\kappa_L}{3}\sum_{ij}\left(\frac{{\rm Im}\,X_{\rm eff}^{ij}}{\lambda^5}\right)^2, \tag{16.118}$$

where all the quantities κ_+, κ_L and $P_c(X)$ are the same as in the SM. The last diagram in Figure 16.1 is relevant for charm meson decays.

Downloaded from https://www.cambridge.org/core. UNIVERSIDAD AUTONOMA METROPOLITANA, on 16 Nov 2026 at 12:03:57, subject to the Cambridge Core terms of use, available at https://www.cambridge.org/core/terms. https://doi.org/10.1017/9781139524100.022

16.4.6 U_3

As the model is not renormalizable, we cannot reliably calculate the box diagrams and correspondingly the shifts ΔS, but the structure of various couplings implies

$$\Delta S(K) = \frac{c_K}{4\pi^2}\left[\frac{H^{3L}_{sd}}{\lambda_t^{(K)}}\right]^2 \left[\kappa(U_{3,0}) + 4\,\kappa(U_{3,-})\right] \tag{16.119}$$

and

$$\Delta S(B_q) = \frac{c_q}{4\pi^2}\left[\frac{H^{3L}_{bq}}{\lambda_t^{(q)}}\right]^2 \left[\kappa(U_{3,0}) + 4\,\kappa(U_{3,-})\right] \tag{16.120}$$

with c_i dependent on the UV completion considered. Without it the box diagram is quadratically divergent. The contributions of $U_{3,0}$ and $U_{3,-}$ involve charged leptons and neutrinos, respectively. We give this formula only for curiosity, but it should not be used in phenomenological applications. On the other hand, no loops have to be evaluated to obtain the following formulas. They just result from tree diagrams.

For Y_A we find

$$Y_A(K) = Y_{\rm SM} - \kappa(U_{3,0})\left[\frac{h^{3L}_{s\mu}(h^{3L}_{d\mu})^*}{\lambda_t^{(K)}}\right], \qquad Y_A(B_q) = Y_{\rm SM} - \kappa(U_{3,0})\left[\frac{h^{3L}_{q\mu}(h^{3L}_{b\mu})^*}{\lambda_t^{(q)}}\right], \tag{16.121}$$

and consequently NP contributions to the Wilson coefficients C_9 and C_{10}

$$C_9^{\rm NP} = -\frac{\kappa(U_{3,0})}{\sin^2\vartheta_W}\left[\frac{h^{3L}_{s\mu}(h^{3L}_{b\mu})^*}{\lambda_t^{(s)}}\right], \qquad C_{10}^{\rm NP} = -C_9^{\rm NP}. \tag{16.122}$$

The relevant functions X^{ij} are this time given by

$$X^{ij}(K) = X_{\rm SM}\delta_{ij} + 2\,\kappa(U_{3,-})\left[\frac{h^{3L}_{s\nu_i}(h^{3L}_{d\nu_j})^*}{\lambda_t^{(K)}}\right] \tag{16.123}$$

and

$$X^{ij}(B_q) = X_{\rm SM}\delta_{ij} + 2\,\kappa(U_{3,-})\left[\frac{h^{3L}_{q\nu_i}(h^{3L}_{b\nu_j})^*}{\lambda_t^{(q)}}\right]. \tag{16.124}$$

16.4.7 $\tilde{R}_2$

For the shifts ΔS we find

$$\Delta S(K) = \frac{\tilde{r}}{16\pi^2}\left[\frac{\tilde{H}^{2L}_{sd}}{\lambda_t^{(K)}}\right]^2 \left[\kappa(\tilde{R}_2^+) + \kappa(\tilde{R}_2^-)\right] \tag{16.125}$$

Downloaded from https://www.cambridge.org/core. UNIVERSIDAD AUTONOMA METROPOLITANA, on 16 Nov 2026 at 12:03:57, subject to the Cambridge Core terms of use, available at https://www.cambridge.org/core/terms. https://doi.org/10.1017/9781139524100.022

and

$$\Delta S(B_q) = \frac{\tilde{r}}{16\pi^2}\left[\frac{\tilde{H}^{2L}_{bq}}{\lambda_t^{(q)}}\right]^2 \left[\kappa(\tilde{R}_2^+) + \kappa(\tilde{R}_2^-)\right]. \tag{16.126}$$

The contributions of $\tilde{R}_2^+$ and $\tilde{R}_2^-$ involve charged leptons and neutrinos, respectively.

For Y_A we find

$$Y_A(K) = Y_{\rm SM} - \frac{\kappa(\tilde{R}_2^+)}{2}\left[\frac{\tilde{h}^{2L}_{s\mu}(\tilde{h}^{2L}_{d\mu})^*}{\lambda_t^{(K)}}\right], \qquad Y_A(B_q) = Y_{\rm SM} - \frac{\kappa(\tilde{R}_2^+)}{2}\left[\frac{\tilde{h}^{2L}_{q\mu}(\tilde{h}^{2L}_{b\mu})^*}{\lambda_t^{(q)}}\right]. \tag{16.127}$$

Equivalently we find for the Wilson coefficients C_9' and C_{10}'

$$C_9' = -\frac{\kappa(\tilde{R}_2^+)}{2\sin^2\vartheta_W}\left[\frac{\tilde{h}^{2L}_{s\mu}(\tilde{h}^{2L}_{b\mu})^*}{\lambda_t^{(s)}}\right], \qquad C_{10}' = -C_9'. \tag{16.128}$$

There are no NP contributions to C_9 and C_{10}. In writing the shifts in (16.127), we took into account that NP contributions come from right-handed currents, which implies the minus sign in the shift in Y_A if it is inserted in the SM expressions. This flip of the sign should not be made in evaluating C_9' and C_{10}' as it is taken into account already in the operators.

The relevant functions X^{ij} are

$$X^{ij}(K) = X_{\rm SM}\delta_{ij} - \frac{\kappa(\tilde{R}_2^-)}{2}\left[\frac{\tilde{h}^{2L}_{s\nu_i}(\tilde{h}^{2L}_{d\nu_j})^*}{\lambda_t^{(K)}}\right] \tag{16.129}$$

and

$$X^{ij}(B_q) = X_{\rm SM}\delta_{ij} - \frac{\kappa(\tilde{R}_2^-)}{2}\left[\frac{\tilde{h}^{2L}_{q\nu_i}(\tilde{h}^{2L}_{b\nu_j})^*}{\lambda_t^{(q)}}\right]. \tag{16.130}$$

We now turn our attention to two models in which, as seen in Table 16.4, there are no tree-level contributions to processes with neutrinos in the final state. This avoids constraints from such processes but could be problematic if one day NA62 experiment will find NP in $K^+ \to \pi^+\nu\bar{\nu}$, KOTO in $K_{\rm L} \to \pi^0\nu\bar{\nu}$, and Belle II experiment in $b \to s\nu\bar{\nu}$ transitions.

16.4.8 U_1

Proceeding as in the case of the U_3 model, we first find from the box diagram in Figure 16.2, involving either only left-handed or only right-handed couplings, the shifts in $\Delta S(B_q)$

$$\Delta S(B_q) = \frac{c}{4\pi^2}\kappa(U_1)\left(\left[\frac{H^{1L}_{bq}}{\lambda_t^{(q)}}\right]^2 + \left[\frac{H^{1R}_{bq}}{\lambda_t^{(q)}}\right]^2\right), \tag{16.131}$$

with c dependent on the UV completion considered

Downloaded from https://www.cambridge.org/core. UNIVERSIDAD AUTONOMA METROPOLITANA, on 16 Nov 2026 at 12:03:57, subject to the Cambridge Core terms of use, available at https://www.cambridge.org/core/terms. https://doi.org/10.1017/9781139524100.022

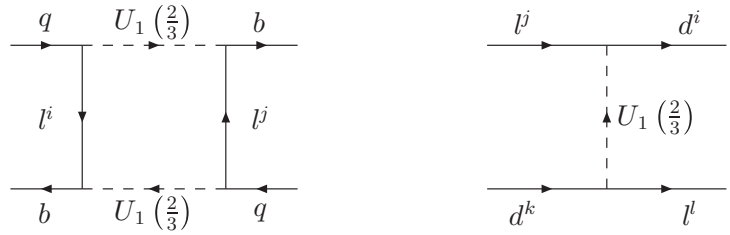


Figure 16.2 Left: Contribution to $B_q^0 - \bar{B}_q^0$ mixing in the U_1 model. Right: Contribution to semileptonic decay.

But the dominant is the box diagram in Figure 16.2 when both LH and RH couplings are present. It contributes to the Wilson coefficient of the operator $Q_2^{\rm LR}$ that has enhanced matrix elements, in particular in the K system. For $B_s^0 - \bar{B}_s^0$ mixing we find

$$\Delta H_{\rm eff} = -\frac{1}{2\pi^2}\frac{c}{m_{\rm LQ}^2} H_{bs}^{1L} H_{bs}^{1R} Q_2^{\rm LR}, \tag{16.132}$$

where the operator $Q_2^{\rm LR}$ is defined in (13.8). Again c depends on the UV completion. Analogous expressions are found for $B_d^0 - \bar{B}_d^0$ and $K^0 - \bar{K}^0$ mixings.

Next, the second diagram in Figure 16.2, with (LH,LH), (RH,RH), (LH,RH), and (RH,LH) combinations of couplings, generates four diagrams and after proper Fierz transformations the following contributions to the Wilson coefficients relevant for $b \to s\mu^+\mu^-$ transitions:

$$C_9^{\rm NP} = -\frac{\kappa(U_1)}{\sin^2\vartheta_W}\left[\frac{h_{s\mu}^{1L}(h_{b\mu}^{1L})^*}{\lambda_t^{(s)}}\right], \qquad C_{10}^{\rm NP} = -C_9^{\rm NP}, \tag{16.133}$$

$$C_9' = -\frac{\kappa(U_1)}{\sin^2\vartheta_W}\left[\frac{h_{s\mu}^{1R}(h_{b\mu}^{1R})^*}{\lambda_t^{(s)}}\right], \qquad C_{10}' = C_9', \tag{16.134}$$

$$m_b C_S = 2\frac{\kappa(U_1)}{\sin^2\vartheta_W}\left[\frac{h_{s\mu}^{1L}(h_{b\mu}^{1R})^*}{\lambda_t^{(s)}}\right], \qquad C_P = -C_S, \tag{16.135}$$

$$m_b C_S' = 2\frac{\kappa(U_1)}{\sin^2\vartheta_W}\left[\frac{h_{s\mu}^{1R}(h_{b\mu}^{1L})^*}{\lambda_t^{(s)}}\right], \qquad C_P' = C_S'. \tag{16.136}$$

As we will see later, the U_1 model appears presently to be the favorite LQ model. This motivated various authors to perform detailed analyses of collider signatures of this LQ that in a large class of ultraviolet complete models appears together with Z' and color-octet G'. We refer to a very recent analysis in [1055], where references to other analyses can be found. We will still encounter this model at several stages of our expedition.

16.4.9 R_2

For the shifts ΔS we find

$$\Delta S(K) = \frac{\tilde{r}}{16\pi^2}\left[\frac{H_{sd}^{2R}}{\lambda_t^{(K)}}\right]^2 \kappa(R_2^-) \tag{16.137}$$

Downloaded from https://www.cambridge.org/core. UNIVERSIDAD AUTONOMA METROPOLITANA, on 16 Nov 2026 at 12:03:57, subject to the Cambridge Core terms of use, available at https://www.cambridge.org/core/terms. https://doi.org/10.1017/9781139524100.022

and

$$\Delta S(B_q) = \frac{\tilde{r}}{16\pi^2}\left[\frac{H_{bq}^{2R}}{\lambda_t^{(q)}}\right]^2 \kappa(R_2^-). \tag{16.138}$$

For Y_A function

$$Y_A(K) = Y_{\rm SM} + \frac{\kappa(R_2^-)}{2}\left[\frac{h_{s\mu}^{2R}(h_{d\mu}^{2R})^*}{\lambda_t^{(K)}}\right], \qquad Y_A(B_q) = Y_{\rm SM} + \frac{\kappa(R_2^-)}{2}\left[\frac{h_{q\mu}^{2R}(h_{b\mu}^{2R})^*}{\lambda_t^{(q)}}\right]. \tag{16.139}$$

Moreover,

$$C_9^{\rm NP} = -\frac{\kappa(R_2^-)}{2\sin^2\vartheta_W}\left[\frac{h_{s\mu}^{2R}(h_{b\mu}^{2R})^*}{\lambda_t^{(s)}}\right], \qquad C_{10}^{\rm NP} = C_9^{\rm NP}, \qquad C'_{10} = C'_9 = 0. \tag{16.140}$$

Note that RH and not LH couplings enter $C_{9,10}^{\rm NP}$. It is a good practice to verify this and also to calculate LQ contributions to $D^0 - \bar{D}^0$ mixing in this model, which are dominated by the operator $Q_2^{\rm LR}$.

As we will see soon, this model at first sight cannot help in explaining the B physics anomalies because at tree-level it implies the relation between the shifts in the Wilson coefficients given in (16.140), which disagrees with the successful one in (12.1).

The solution to this problem proposed in [1056] is to simply set the relevant Yukawa coupling to zero so that the transition $b \to s\ell^+\ell^-$ is absent at tree-level, and it takes place first at one-loop level. The box diagram with the exchange of the W boson, top-quark, and the leptoquark with charge +5/3 allows then to satisfy the second relation in (12.1). In this manner the $R(K)$ and $R(K^*)$ anomalies can be explained. A similar idea was used in [1057] in the case of the S_1 leptoquark, which does not contribute to $b \to s\ell^+\ell^-$ at tree-level. While at first sight this model looked like being useful for the explanation of the $R(K)$ anomaly, the induced problems elsewhere made it phenomenologically unviable [1048].

The model suggested in [1056] is still viable as far as $R(K)$ and $R(K^*)$ are concerned, but in contrast to the U_1 model cannot explain $R(D)$ and $R(D^*)$ anomalies [538]. We refer to [1056] for detailed calculations in this model. Subsequently, it has been demonstrated in [1058] that R_2 model with flavor anomalies generated at one-loop level can not only explain the $R(K)$ and $R(K^*)$ anomalies but also the $(g-2)_\mu$ anomaly and the IceCube data [1059] on the sterile neutrinos. For a recent analysis of IceCube data in S_1 and U_1 models, see [1060].

16.4.10 Remaining LQ Models

For completeness we want to list some general properties of the remaining five models and refer to the literature where detailed phenomenological analyses of most of them can be found. The collection of some of these properties can be found in Table 16.4, and others can be deduced from the Lagrangians listed earlier. They are

- The leptoquarks S_1, and V_2, similar to U_1 and R_2, have both left-handed and right-handed couplings and can provide through left-right operators more important contributions to

Downloaded from https://www.cambridge.org/core. UNIVERSIDAD AUTONOMA METROPOLITANA, on 16 Nov 2026 at 12:03:57, subject to the Cambridge Core terms of use, available at https://www.cambridge.org/core/terms. https://doi.org/10.1017/9781139524100.022

$\Delta F = 2$ observables than is the case of other models in which such operators are absent. In this context U_1 and V_2 are relevant for $K^0 - \bar{K}^0$ and $B_{s,d} - \bar{B}_{s,d}$ mixings, while S_1 and R_2 for $D^0 - \bar{D}^0$ mixing.

- These four models can also be distinguished from each other by their couplings to leptons. S_1 does not contribute to $b \to s\ell^+\ell^-$ transitions but has an impact on decays of K and $B_{s,d}$ with neutrinos in the final state. The opposite is true for R_2 and U_1. On the other hand, V_2 provides contributions to all these decays.
- The leptoquark $\tilde{S}_1$ is rather special as it only couples to charged leptons and down-quarks. As such it predicts no NP contributions to $K^+ \to \pi^+\nu\bar{\nu}$, $K_L \to \pi^0\nu\bar{\nu}$, $b \to s\nu\bar{\nu}$ transitions and charm physics. On the other hand, it contributes to $b \to s\ell^+\ell^-$. Having only one coupling it is more predictive than the remaining models not considered by us in detail but at the end, it is not useful for B physics anomalies and decays with neutrinos in the final state.
- The leptoquarks $\tilde{U}_1$ and $\tilde{V}_2$ are less interesting than other models as they only give contributions to charm observables. Therefore they cannot help with B physics anomalies nor with the ε'/ε anomaly. But possibly they could address the CP violation in charm decays mentioned at the end of Chapter 11.

16.4.11 LQ Models and B Physics Anomalies

General View

In Chapter 12 we have mentioned various anomalies, and we will return to them again in Chapter 18, where we will compare various explanations of them. In particular LQs provide a very natural description of lepton flavor universality violation (LFUV), as due to $\mu \to e\gamma$ constraint they should have small couplings to electrons.

Here we would like to concentrate on LQ models recalling that the two most favorite solutions obtained in various global analyses of $b \to s\ell^+\ell^-$ [494, 721] turned out before Moriond 2019 to be

$$i)\ C_9^{\rm NP} < 0, \qquad ii)\ C_9^{\rm NP} = -C_{10}^{\rm NP} < 0. \tag{16.141}$$

While these solutions, as reported in Chapter 12, are even after Moriond 2019 among the favored ones, other possible solutions involving several WCs become competitive and even superior to them. We will return to them later, but let us first find out how different LQ models face the solutions in (16.141). We identify the following relations

$$C_9^{\rm NP} = -C_{10}^{\rm NP}, \qquad (S_3, U_1, U_3) \tag{16.142}$$

$$C_9' = -C_{10}', \qquad (\tilde{R}_2, V_2) \tag{16.143}$$

$$C_9^{\rm NP} = C_{10}^{\rm NP}, \quad (R_2, V_2) \qquad C_9' = C_{10}', \quad (\tilde{S}_1, U_1) \tag{16.144}$$

$$C_P = -C_S \quad (U_1, V_2) \qquad C_P' = C_S', \quad (U_1, V_2) \tag{16.145}$$

Downloaded from https://www.cambridge.org/core. UNIVERSIDAD AUTONOMA METROPOLITANA, on 16 Nov 2026 at 12:03:57, subject to the Cambridge Core terms of use, available at https://www.cambridge.org/core/terms. https://doi.org/10.1017/9781139524100.022

and recall that in the S_1 model there are no contributions to $b \to s\ell^+\ell^-$ at tree-level. The following observations should be made:

- The first solution in (12.1) in which NP is only present in C_9 cannot be generated with a single leptoquark representation. But it can be generated, e.g., by adding scalar representations R_2 and S_3 [1053].
- The second solution $C_9^{\rm NP} = -C_{10}^{\rm NP}$ is the most natural solution for LQs and can be obtained with a single representation: either S_3 or U_1 [778, 779, 1061–1064]. Also U_3 satisfies this relation.
- On the other hand, LQ models with only right-handed currents, like $\tilde{R}_2$, considered in detail in [1047, 1065] before $R(K^*)$ was measured, are disfavored because in these models $R(K) < 1$ implies $R(K^*) > 1$ or $R(K^*) < 1$ implies $R(K) > 1$ [609, 1066] in disagreement with data, even after Moriond 2019.

Thus as far as $b \to s\ell^+\ell^-$ anomalies are concerned, in the context of LQ models the solution $C_9^{\rm NP} = -C_{10}^{\rm NP}$ is the favorite one. But the question arises how these models face the $R(D)$ and $R(D^*)$ anomalies. Here a solution to these anomalies can be achieved with NP contribution to the operator $(\bar{c}_L\gamma_\mu b_L)(\bar{\tau}_L\gamma_\mu \nu_L)$. This is consistent with B_c lifetime [571] and q^2 distributions [541, 549, 574] in these decays in contrast to models like 2HDM, in which one attempts to explain the anomalies with scalar and pseudoscalar mediators. Assuming then $\mathrm{SU}(2)_L$ gauge invariance, these anomalies are not only correlated with the ones in $b \to s\ell^+\ell^-$ but have also implications for $b \to s\tau^+\tau^-$, which must be significantly enhanced, and this is also the case of $b \to s\nu\bar{\nu}$. We have discussed this in detail in Section 14.5.

In a general analysis the bounds from $B \to K^{(*)}\nu\bar{\nu}$ can be avoided if NP couples dominantly to third generation. But this disagrees with direct LHC searches [1067] and electroweak precision tests [765]. Introducing more operators and assuming special flavor structure, one can with some tuning avoid these constraints as demonstrated in [719]. But within the LQ models the difficulty with $b \to s\nu\bar{\nu}$ transitions can be avoided easily in the U_1 model in which the coefficients $C_{lq}^{(1)}$ and $C_{lq}^{(3)}$ in the SMEFT satisfy the relation $C_{lq}^{(1)} = C_{lq}^{(3)}$. In this case, as seen in (14.79), at the LQ scale there are no contributions to $b \to s\nu\bar{\nu}$ at the tree-level [778, 779]. Also in the R_2 model tree-level contributions to processes with neutrinos in the final state are absent. This is not the case of S_3 and U_3, which are very constrained by these transitions.

The absence of tree-level contributions to $b \to s\nu\bar{\nu}$ and also $K^+ \to \pi^+\nu\bar{\nu}$ and $K_{\rm L} \to \pi^0\nu\bar{\nu}$ at tree-level in the U_1 and R_2 models at the matching scale allows to avoid the constraints from these decays, which are generally problematic for LQ models. But if future data will require significant NP contributions to them, the fate of these models will depend on whether the RG effects generating such contributions will be able to fit the data [667]. We will return to this issue in Section 16.4.13. The fate of the U_1 model, as far as $\Delta F = 2$ observables are concerned, can only be answered after some UV completion is constructed. But as in this model both left-handed and right-handed couplings are present, possibly future anomalies in nonleptonic observables could be easier solved than in S_3, U_3, and $\tilde{R}_2$ models. One of the reasons is the increase of free-parameters. Another is the

Downloaded from https://www.cambridge.org/core. UNIVERSIDAD AUTONOMA METROPOLITANA, on 16 Nov 2026 at 12:03:57, subject to the Cambridge Core terms of use, available at https://www.cambridge.org/core/terms. https://doi.org/10.1017/9781139524100.022

Table 16.5 Selected references to specific LQ models.

LQ representation	References	Comments (see text)
S_1	[1057, 1068–1070]	R_K, $R(D)$, $R(D^*)$, $(g-2)_\mu$
S_1 and $\tilde{R}_2$	[1071]	Charged and neutral, ν-masses
R_2	[1072]	Charged and neutral
R_2, loop	[1056, 1058, 1068]	R_K, R_{K^*}, $(g-2)_\mu$, IceCube event.
$\tilde{R}_2$, loop	[1047, 1073]	R_K and $R(D)$
S_1 and S_3	[593, 719, 1052, 1098]	Charged and neutral
S_3 and $\tilde{R}_2$	[1053, 1071]	Charged and neutral
R_2 and $\tilde{R}_2$	[1074, 1075]	Charged and neutral
S_3 and R_2	[849]	Charged and neutral
S_1, R_2, S_3	[1076]	EDMs
U_1	[719, 945, 1052, 1064, 1077–1079]	R_K and $R(D)$ and $R(D^*)$
U_1	[1080–1082]	Gauge LQ
U_1	[1083]	Composite LQ
V_2	[1084]	Neutral
U_3	[944, 1063, 1078]	General analysis
U_3	[1061]	Strong dynamics
(U_1, U_3)	[945, 1085]	R_K and $R(D)$ and $R(D^*)$
(U_1, U_3, S_3)	[729]	$R(K)$ and $R(K^*)$
$\tilde{U}_1$ and R_2	[1086]	Neutral

generation of left-right operators, which as we will see later could help to explain the ε'/ε-anomaly. On the other hand left-right operators provide enhanced NP contributions to ΔM_K and ε_K so that possibly some tuning of parameters will be required to satisfy all constraints. In the U_1 model also new operators to $b \to s\mu^+\mu^-$ contribute, in particular $Q_S^{(\prime)}$ and $Q_P^{(\prime)}$, but their Wilson coefficients must be small for the model to agree with $B_s \to \mu^+\mu^-$ data. Similar comments, as far as left-right operators are concerned, apply also to the R_2 model. We will return to some of these issues in the context of UV completions later.

In Table 16.5 we collect selected papers on various LQ models. As I cannot discuss them here in detail, but some of these papers could turn out to be useful for future model building, I will just make a few comments on them. One should realize that some anomalies could go away, and the pattern of anomalies could change in the future, opening thereby the road for models that are not favored in 2019. The ideas presented in the papers listed in Table 16.5 could, however, still turn out to be useful for the construction of new models. The description of these papers presented here has also a historical value, showing a big excitement of theorists in the presence of deviations from the SM predictions.

The neutral anomaly ($b \to s\mu^+\mu^-$) has been discussed extensively in models with several LQ representations in [729]. Tables I and II in this paper show relations between C_9 and C_{10} and also between $R(K)$ and $R(K^*)$. The authors favor (U_1, U_3, S_3) as expected from our comments earlier.

Downloaded from https://www.cambridge.org/core. UNIVERSIDAD AUTONOMA METROPOLITANA, on 16 Nov 2026 at 12:03:57, subject to the Cambridge Core terms of use, available at https://www.cambridge.org/core/terms. https://doi.org/10.1017/9781139524100.022

I found the paper [945] very useful. The authors look at $R(K)$, $R(D)$, and $R(D^*)$ anomalies, which they studied already in [777] and compare a model with a vector boson triplet with the U_1 LQ model giving arguments for the superiority of U_1. In this context they review previous analyses in SMEFT [778, 779], in which it is shown that among S_3, U_1, and U_3 only U_1 can simultaneously explain neutral and charged anomalies while satisfying other constraints, in particular from $b \to s\nu\bar{\nu}$ transitions.

One should, however, note that [945] appeared before the $R(K^*)$ anomaly has been announced. Taking the latter anomaly into account, it has been found in [1078] that U_1, U_3, and S_3 models cannot simultaneously explain $R(K)$, $R(K^*)$, $R(D)$, and $R(D^*)$ anomalies within 1σ. But with the new data on $R(D)$ and $R(D^*)$ from Belle the situation changed, and in particular the U_1 model performs better than previously.

Next, it has been demonstrated in [1049] that none of the *scalar* LQs of mass $m_{\rm LQ} \approx 1$ TeV can alone accommodate simultaneously $R(K)$, $R(K^*)$, $R(D)$, and $R(D^*)$ anomalies when constraints arising from both low-energy observables and from direct searches at the LHC are taken into account. It appears then that the only single LQ scenario that works for $m_{\rm LQ} \approx$ 1–2 TeV is the vector LQ U_1. Otherwise models with two scalar LQs, as listed in Table 16.5, have to be considered. A general analysis of constraints on scalar LQs from lepton and kaon physics can be found in [1346]. Effects of scalar LQs in $B \to \mu\bar{\nu}$ are discussed in [1345].

In [1087] a general LQ analysis correlating neutral anomalies with LFV in pure leptonic decays and semileptonic B decays has been performed. Also implications for $\mu \to e\gamma$ have been presented. This paper contains useful formulas for a number of observables. A solution to B physics anomalies is provided by a combination of two scalar LQs S_1 and S_3 [719, 1052], which allows to avoid $b \to s\nu\bar{\nu}$ constraints. Large effects in $b \to s\tau^+\tau^-$, like $\mathcal{B}(B \to \tau^+\tau^-)$ of $O(10^{-3})$, are predicted to be compared with $O(10^{-6})$ in the SM.

In [849] another solution to B physics anomalies with two scalar representations has been proposed. This time S_3 and R_2 explain $R(K^{(*)})$ and $R(D^{(*)})$ anomalies, respectively. It is a UV complete model based on SU(5) Grand Unified Theory. Certainly, an interesting paper.

In [1064] a study of flavor symmetry $\mathrm{U}(2)^5$ in LQ models has been investigated. It is assumed that LQs couple first only to third generation. The remaining couplings are generated in the process of the breakdown of the symmetry. Considering U_1, S_3, U_3 it is concluded in agreement with [778, 779] that U_1 should be favored. In [719] both charged and neutral anomalies in an EFT-framework based on $\mathrm{U}(2)_q \times \mathrm{U}(2)_l$ symmetry have been studied with couplings predominantly to third generation of left-handed quarks and leptons. LQs in different representations under the $\mathrm{SU}(2)_L$ and colorless vector $\mathrm{SU}(2)_L$-triplets (W', B') have been considered, and again the U_1 model has been declared as a winner, although the model with S_1 and S_3, discussed in [1052, 1098], provides also the explanation of all B physics anomalies while satisfying other constraints without fine-tuning.

In models considered in [719] it is shown that the constraints from direct LHC searches and electroweak precision tests pointed out in [1067] and [765], respectively, can be presently avoided through a particular flavor structure that allows to explain anomalies with higher LQ masses than required in the construction in [765, 1067]. The paper [719], known in the flavor community as the "Zürich guide," can be strongly recommended. See also [1319].

Downloaded from https://www.cambridge.org/core. UNIVERSIDAD AUTONOMA METROPOLITANA, on 16 Nov 2026 at 12:03:57, subject to the Cambridge Core terms of use, available at https://www.cambridge.org/core/terms. https://doi.org/10.1017/9781139524100.022

At this stage it should be again stressed that having explicit models like LQ models, Z' models, and other simplified models discussed in the previous chapter has some advantage over pure EFT approach. Indeed, complementing EFT approaches with appropriate simplified models with new heavy mediators is essential [944, 1064], if one wants to address the compatibility of models addressing present anomalies with other low-energy constraints and with high-p_T data. Due to the relatively low scale of NP required for the explanations of the charged-current anomalies, high-p_T constraints are very relevant [1044, 1055, 1067, 1088–1093].

UV Completions

The fact that the U_1 model with a vector LQ seems to be the favorite LQ model, but is not renormalizable, motivated a number of authors to look for UV completions in which the vector LQ is a gauge boson. In this context most popular are models involving Pati–Salam group $\mathrm{SU}(4) \times \mathrm{SU}(2)_L \times \mathrm{SU}(2)_R$. In this construction proton remains stable in contrast to several LQ models. We refer to [935, 1080–1082, 1094] for details. See also [849, 1095–1104].

Although the Pati–Salam group is present in all models of this type, some papers invoke larger groups and include additional new particles. Here we provide an express review of some of these papers.

- In [1080] Pati–Salam gauge group $\mathrm{SU}(4) \times \mathrm{SU}(2)_L \times \mathrm{SU}(2)_R$ is considered and both charged and neutral anomalies are explained as well as $(g-2)_\mu$ anomaly. The model contains also vector-like fermions.
- In [1081] the authors study the gauge group $\mathrm{SU}(4) \times \mathrm{SU}(3)' \times \mathrm{SU}(2)_L \times \mathrm{U}(1)'$. See also the papers [1055, 1089, 1100, 1105]. In fact, as stressed in [1055, 1081] this is the minimal gauge group containing the U_1 as a gauge boson, which fulfills the necessary requirements to provide a successful explanation of the anomalies while remaining consistent with high-p_T data.
- A larger gauge group, that involves the product of three Pati–Salam groups was proposed in [1082] with the goal to explain not only flavor anomalies but also the pattern of fermion masses and CKM parameters (see also [1095, 1099]). In contrast to [1055, 1089, 1100, 1105] in this model the gauge group is nonuniversal among the different SM-like families. For an earlier paper by these authors on a general EFT with $\mathrm{U}(2)^n$ flavor symmetry, see [1106], where it has been pointed out that the correlation between $K \to \pi\nu\bar{\nu}$, $B \to \pi\nu\bar{\nu}$, and $R(D^*)$ could distinguish between various NP scenarios. A very interesting paper in this context is also [1107], the generalization of the model in [1082] to include RH couplings of the U_1 LQ. This is motivated by the Moriond 2019 news that possibly $R(K) \neq R(K^*)$ and distinguishes this analysis from other analyses of B physics anomalies in which only LH couplings of the U_1 LQ have been kept.[1] I think this is an interesting direction even if the number of gauge bosons and free parameters is large in these models. See also [1316].

[1] The presence of both LH and RH couplings in the U_1 model is crucial for addressing the ε'/ε anomaly in this model as pointed out earlier in [667] and discussed in Section 16.4.13.

Downloaded from https://www.cambridge.org/core. UNIVERSIDAD AUTONOMA METROPOLITANA, on 16 Nov 2026 at 12:03:57, subject to the Cambridge Core terms of use, available at https://www.cambridge.org/core/terms. https://doi.org/10.1017/9781139524100.022

- In [1100] the Pati–Salam group has been incorporated into the Randall–Sundrum scenario. Breaking the gauge group by boundary conditions the resulting massive vector LQ has the same mass scale as the vector-like fermions and other resonances present in this model. $R(K)$ and $R(K^*)$ anomalies can easily be explained in this model. One also finds sizable effects in $R(D)$, $R(D^*)$, and $R(J/\psi)$, but the model could not account for their central values prior to Moriond 2019 due to stringent constraints from $D^0 - \bar{D}^0$ mixing and $\tau \to 3\mu$. The situation improved after Moriond 2019 so that within 2σ the model is consistent with new $R(D)$ and $R(D^*)$ values in Table 9.1. Also, addition of RH couplings, increasing the effect by scalar operators in $R(D)$ and $R(D^*)$, would help.
- In [933, 934] solutions to B physics anomalies within some other nonabelian groups have been proposed.

While, the virtue of concrete simplified Z' and LQ models over EFT has already been mentioned earlier, the most important consequence following from the requirement of a consistent UV completion is the necessity of extra particles, with interesting high-p_T signatures that cannot be deduced within the simplified model [1107]. In the latter paper these new states include both a color-octet (G') and a color singlet (Z') vector field, as extensively discussed in [1081, 1082, 1095, 1099], and a pair of vector-like quarks and leptons. Also as pointed out in [1097], the $\Delta F = 2$ constraints imply that the vector-like leptons are likely to be the lightest exotic states. In my view this is an interesting direction, as it is hard to imagine that NP consists of a single LQ, even as successful as the U_1.

Still another idea is to explain B physics anomalies via composite Higgs model, in which both Higgs and the S_3 LQ arise as pseudo-Goldstone bosons of a strong dynamics [1061]. Fermion masses are assumed to be generated via the mechanism of partial compositeness, which largely determines the LQ couplings increasing the predictive power of the model. Also nonuniversal lepton interactions are implied naturally in this manner.

The impact of flavor symmetries on the explanations of B physics anomalies in general context and in LQ models has been studied in [1062]. Analyses as the ones in [774, 1061, 1062, 1108] and also in [1082, 1095, 1099, 1106]), mentioned already earlier, could provide valuable information on flavor symmetries beyond the SM when the data improves. This is also evident from an interesting analysis in [774], which demonstrates how some assumptions about flavor dynamics at short-distance scales could provide correlations between B, K, and D physics as well as collider physics, which go beyond MFV and $U(2)^3$ symmetry.

On the other hand, the investigation of scalar leptoquarks accommodating the B-physics anomalies in the context of GUTS is another interesting avenue. See [849] and references to earlier papers therein. Vector leptoquarks in the context of GUTS are discussed in [1109].

As we have seen, some of LQ scenarios are able to address simultaneously the $b \to s\ell\ell$ anomalies as well as the hints for LFUV in $R(D^{(*)})$ [719, 769, 849, 945, 1052, 1057, 1081–1083, 1095, 1100, 1110, 1111]. However, such models are strongly constrained by measurements of the $\tau^+\tau^-$ invariant mass spectrum at the LHC as already pointed out in [1067] and by existing bounds on $B \to K\nu\nu$ and $B \to K^*\nu\nu$ from BaBar and Belle, by existing bounds on LFV tau decays like $\tau \to 3\mu$, from precision measurements of the

Downloaded from https://www.cambridge.org/core. UNIVERSIDAD AUTONOMA METROPOLITANA, on 16 Nov 2026 at 12:03:57, subject to the Cambridge Core terms of use, available at https://www.cambridge.org/core/terms. https://doi.org/10.1017/9781139524100.022

leptonic couplings of the Z at LEP [765, 767, 1112], and by lepton-universality tests in leptonic tau decays $\tau \to \ell \nu_\tau \bar{\nu}_\ell$ [765, 767, 1112].

It appears to me that not all of these constraints have been taken into account in several papers listed earlier because such analysis is very involved, in particular if RG effects within SMEFT are taken into account. Therefore the codes listed in Chapter 14 turn out to be an invaluable help here.

In this context the analysis in [516], which uses these codes extensively, is important. Considering a multitude of observables this analysis demonstrates again the importance of taking into account loop-effects, both in the RG running and in the matching, as emphasized already in [743, 765, 767]. In particular analyzing the U_1 model the authors of [516] demonstrated that an additional flavor universal shift in C_9, as considered by several authors, can be generated through RG effects from four-fermion operators above the electroweak scale. In this context, as pointed out already in [743], semitautonic operators involving $b \to c$ transitions are most interesting as they allow a simultaneous explanation of $R(D)$ and $R(D^*)$ anomalies. Such effect has been pointed out earlier in [742].

Finally, we recommend a number of analyses devoted to $b \to c\tau\bar{\nu}_\tau$ transitions after Moriond 2019 data that we discussed already in Section 9.4. These are [552–556], which again are dominated by LQ models.

16.4.12 LQ Models and MFV

There is an interesting question whether imposing MFV on LQ models could still allow for the explanation of $R(K)$ and $R(K^*)$. This question has been addressed in [1113]. To this end the charged lepton Yukawa matrix has been taken as the only spurion that violates lepton flavor universality. It has been found that a combination of constraints from $b \to s\mu^+\mu^-$, $b \to s\tau^+\tau^-$, $b \to s\nu\bar{\nu}$, $b\bar{b} \to \tau^+\tau^-$, $b \to c\tau\nu$ transitions, and for scalar LQs from $B_s - \bar{B}_s$ mixing excludes MFV in these models. A similar conclusion has been reached in [1114].

It should be noted that B physics anomalies do not require new complex phases but as shown in these papers already the MFV flavor structure cannot be imposed in LQ models if one wants to understand these anomalies in these models. But MFV is quite generally much stronger violated through the ε'/ε-anomaly. Let us then turn our attention to the ratio ε'/ε within the LQ models.

16.4.13 LQ Models and ε'/ε Anomaly

We have seen in the previous chapter and also in this one that several NP scenarios are able to provide sufficient upward shift in ε'/ε and obtain agreement with experiment. These include in particular tree-level Z' exchanges with explicit realization in 331 models [852, 853] or models with tree-level Z exchanges [766, 799] with explicit realization in models with mixing of heavy vector-like fermions with ordinary fermions [666] and Littlest Higgs model with T-parity [850]. Also simplified Z' scenarios [601, 851] and the MSSM [857] are of help here. As we have just discussed, LQ models are rather successful in addressing B-physics anomalies, which some of the scenarios listed earlier are not able to do. The question then arises how LQs face the ε'/ε anomaly.

Downloaded from https://www.cambridge.org/core. UNIVERSIDAD AUTONOMA METROPOLITANA, on 16 Nov 2026 at 12:03:57, subject to the Cambridge Core terms of use, available at https://www.cambridge.org/core/terms. https://doi.org/10.1017/9781139524100.022

Already from the beginning one can expect that the ε'/ε anomaly will be a challenge for those LQ analyses of B-physics anomalies in which all NP couplings have been chosen to be real and those to the first generation set to zero. It should also be realized that the anomalies $R(D)$ and $R(D^*)$, although being very significant, can still be explained in some LQ models through a tree-level LQ exchange. On the other hand, the ε'/ε anomaly, being even larger, if the bound on ε'/ε in [244, 245] is assumed, can only be addressed in these models at one-loop level. This shows that the hinted ε'/ε anomaly is a big challenge for LQ models.

These expectations have been confirmed by a very detailed analysis in [667]. Assuming a mass gap to the EW scale, the main mechanism for LQs to contribute to ε'/ε turns out to be EW gauge-mixing of semileptonic into nonleptonic operators, which is the Scenario V in the context of the SMEFT in Chapter 14. The detailed analysis can be found in [667]. There also one-loop decoupling for scalar LQs has been performed, finding that in all models with both left-handed and right-handed LQ couplings, that is S_1, R_2, and V_2 and U_1, box diagrams generate numerically strongly enhanced EWP operators Q_8 and Q_8' already at the LQ scale. This behavior is rather special for LQs as in most models Q_8 and Q_8' operators cannot be generated at high scale even at NLO and are generated only in QCD RG running to low-energy scales from the operators Q_7 and Q_7', respectively. A good example is the SM and all NP models discussed by us until now.

Investigating correlations of ε'/ε with rare Kaon processes ($K_{\rm L} \to \pi^0\nu\bar{\nu}$, $K^+ \to \pi^+\nu\bar{\nu}$, $K_L \to \pi^0\ell\bar{\ell}$, $K_S \to \mu\bar{\mu}$, ΔM_K, and ε_K), one finds then that even imposing only a moderate enhancement of $(\varepsilon'/\varepsilon)_{\rm NP} = 5 \times 10^{-4}$ to explain the current anomaly leads to conflicts with experimental upper bounds on rare Kaon processes. They exclude all LQ models with only a single coupling as an explanation of the ε'/ε anomaly and put serious constraints on parameter spaces of the models S_1, R_2, and V_2 and U_1, where the box diagrams can in principle provide a rescue to LQ models provided both left-handed and right-handed couplings are nonvanishing. However, then the presence of left-right operators contributing not only to ε'/ε but also to $D^0 - \bar{D}^0$ and $K^0 - \bar{K}^0$ mixings requires some fine-tuning of parameters to satisfy all constraints. In the case of V_2 and U_1 the analysis of box diagrams can only be done in a UV completion.

Future results on $K^+ \to \pi^+\nu\bar{\nu}$ from the NA62 collaboration, $K_{\rm L} \to \pi^0\nu\bar{\nu}$ from the KOTO experiment and $K_S \to \mu\bar{\mu}$ from the LHCb will even stronger exhibit the difficulty of LQ models in explaining the measured ε'/ε, in case the ε'/ε anomaly will be confirmed by improved LQCD calculations. Hopefully also improved measurements of $K_L \to \pi^0\ell\bar{\ell}$ decays will one day help in this context.

The main messages of [667] are then the following ones. If the future improved LQCD calculations will confirm the ε'/ε anomaly at the level $(\varepsilon'/\varepsilon)_{\rm NP} \geq 5 \times 10^{-4}$ LQs are likely not responsible for it. But if the ε'/ε anomaly will disappear one day, large NP effects in rare K decays that are still consistent with present bounds will be allowed. The analysis in [667] is rather involved, and we will not present it here. But it is an excellent arena to practice the technology of SMEFT, which we introduced in Chapter 14, and anybody who wants to test her (his) skills gained in that chapter should study [667] in detail.

Downloaded from https://www.cambridge.org/core. UNIVERSIDAD AUTONOMA METROPOLITANA, on 16 Nov 2026 at 12:03:57, subject to the Cambridge Core terms of use, available at https://www.cambridge.org/core/terms. https://doi.org/10.1017/9781139524100.022